Title: Nitrogen demand, supply, and acquisition strategy control plant responses to elevated CO_2 at different scales

Running Title: N supply and demand control plant responses to CO_2

List of Authors: Evan A. Perkowski[1,*], Ezinwanne Ezekannagha[1], Nicholas G. Smith[1]

Institutional Affiliations: [1]Department of Biological Sciences, Texas Tech University, Lubbock, TX

[*]Corresponding author:
2901 Main St.
Lubbock, TX, 79409
Email: evan.a.perkowski@ttu.edu

ORCIDs: Evan A. Perkowski (0000-0002-9523-8892), Ezinwanne Ezekannagha (0000-0001-7469-949X), Nicholas G. Smith (0000-0001-7048-4387)

Abstract

Plants respond to elevated atmospheric CO_2 concentrations by reducing leaf nitrogen content and photosynthetic capacity – patterns that correspond with increased net photosynthesis rates, total leaf area, and total biomass. Nitrogen supply has been hypothesized to be the primary factor controlling these responses, as nitrogen availability limits net primary productivity globally. Recent work using evo-evolutionary optimality theory suggests that leaf photosynthetic responses to elevated CO_2 are independent of nitrogen supply and are instead driven by leaf nitrogen demand to build and maintain photosynthetic enzymes, which optimizes resource allocation to photosynthetic capacity and maximizes allocation to growth. Here, *Glycine max* L. (Merr) seedlings were grown under two CO_2 concentrations, with and without inoculation with *Bradyrhizobium japonicum*, and across nine soil nitrogen fertilization treatments in a full-factorial growth chamber experiment to reconcile the role of nitrogen supply and demand on leaf and whole-plant responses to elevated CO_2. After seven weeks, elevated CO_2 increased net photosynthesis rates despite reduced leaf nitrogen content and maximum rates of Rubisco carboxylation and electron transport for RuBP regeneration. Effects of elevated CO_2 on net

photosynthesis and indices of photosynthetic capacity were independent of nitrogen fertilization and inoculation. However, positive effects of elevated CO_2 on total biomass and total leaf area were enhanced with increasing nitrogen fertilization due to increased nitrogen uptake and reduced carbon costs to acquire nitrogen. Whole-plant responses to elevated CO_2 were not modified by inoculation across the nitrogen fertilization gradient, as plant investment in nitrogen fixation was similar between CO_2 treatments. These results indicate that leaf nitrogen demand to build and maintain photosynthetic enzymes drives leaf photosynthetic responses to elevated CO_2, while nitrogen supply regulates whole-plant responses. Our findings build on previous work suggesting that terrestrial biosphere models may improve simulations of photosynthetic processes under future novel environments by adopting optimality principles.

Keywords

acclimation, eco-evolutionary optimality, growth chamber, least-cost theory, nitrogen acquisition strategy, photosynthesis, plant functional ecology, whole-plant growth

Introduction

Terrestrial ecosystems are regulated by complex carbon and nitrogen cycles. As a result, terrestrial biosphere models, which are beginning to include coupled carbon and nitrogen cycles (Shi *et al.*, 2016; Davies-Barnard *et al.*, 2020; Braghiere *et al.*, 2022), must accurately represent these cycles under different environmental scenarios to reliably simulate carbon and nitrogen fluxes (Oreskes *et al.*, 1994; Prentice *et al.*, 2015). While the inclusion of coupled carbon and nitrogen cycles in terrestrial biosphere models was intended to improve model reliability, large uncertainty in the role of nitrogen availability and nitrogen acquisition strategy on leaf and whole plant responses to increasing atmospheric CO_2 concentrations persists (Arora *et al.*, 2020; Davies-Barnard *et al.*, 2020; Kou-Giesbrecht *et al.*, 2023), contributing to widespread divergence in future carbon and nitrogen flux simulations across terrestrial biosphere models (Hungate *et al.*, 2003; Friedlingstein *et al.*, 2014; Zaehle *et al.*, 2014; Wieder *et al.*, 2015; Meyerholt *et al.*, 2020).

Over the past few decades, numerous studies have sought to elucidate plant responses to elevated CO_2, revealing consistent leaf and whole-plant patterns. At the leaf level, C_3 plants grown under elevated CO_2 exhibit increased net photosynthesis rates compared to plants grown

under ambient CO_2 (Medlyn *et al.*, 1999; Ainsworth & Long, 2005; Bernacchi *et al.*, 2005; Lee *et al.*, 2011; Poorter *et al.*, 2022). These patterns correspond with reduced mass- and area-based leaf nitrogen content, increased leaf mass per area, reduced stomatal conductance, and reduced photosynthetic capacity, yielding increased photosynthetic nitrogen-use efficiency and water-use efficiency (Curtis, 1996; Drake *et al.*, 1997; Medlyn *et al.*, 1999; Ainsworth & Long, 2005; Ainsworth & Rogers, 2007; Lee *et al.*, 2011; Pastore *et al.*, 2019; Poorter *et al.*, 2022). At the whole-plant level, C_3 plants grown under elevated CO_2 exhibit increased total leaf area, which supports greater net primary productivity and total biomass compared to plants grown under ambient CO_2 (Coleman *et al.*, 1993; Ainsworth *et al.*, 2002; Ainsworth & Rogers, 2007; Finzi *et al.*, 2007; Poorter *et al.*, 2022). Some experiments suggest that elevated CO_2 increases belowground carbon allocation and the ratio of root biomass to shoot biomass compared to plants grown under ambient CO_2 (Nie *et al.*, 2013), though this allocation response is not consistently observed (Luo *et al.*, 1994; Poorter *et al.*, 2022).

Despite consistent plant responses to elevated CO_2 documented across experiments, mechanisms that drive these responses remain unresolved. Some have hypothesized that plant responses to elevated CO_2 are constrained by nitrogen availability, as net primary productivity is limited by nitrogen availability globally (Vitousek & Howarth, 1991; LeBauer & Treseder, 2008; Fay *et al.*, 2015). The progressive nitrogen limitation hypothesis predicts that elevated CO_2 will increase plant nitrogen uptake to support greater net primary productivity, which will cause nitrogen availability to decline over time (Luo *et al.*, 2004). The hypothesis predicts that this response should increase growth and net primary productivity under elevated CO_2 over short time scales that dampen with time as nitrogen becomes progressively more limiting and stored in longer-lived tissues. Growth responses to elevated CO_2 expected from the progressive nitrogen limitation hypothesis have received some support from free-air CO_2 enrichment experiments (Reich *et al.*, 2006; Norby *et al.*, 2010), though these patterns are not consistently observed (Finzi *et al.*, 2006; Moore *et al.*, 2006; Liang *et al.*, 2016).

Assuming positive relationships between soil nitrogen availability, leaf nitrogen content, and photosynthetic capacity (Field & Mooney, 1986; Evans, 1989; Evans & Seemann, 1989; Walker *et al.*, 2014; Firn *et al.*, 2019; Liang *et al.*, 2020), the progressive nitrogen limitation hypothesis implies that reductions in nitrogen availability over time might explain why C_3 plants exhibit decreased leaf nitrogen content and photosynthetic capacity under elevated CO_2.

However, results from free-air CO_2 enrichment experiments show that reductions in leaf nitrogen content and photosynthetic capacity under elevated CO_2 are decoupled from changes in nitrogen availability (Crous *et al.*, 2010; Lee *et al.*, 2011; Pastore *et al.*, 2019). Additionally, variance in leaf nitrogen and photosynthetic capacity across environmental gradients tends to be more strongly determined through aboveground growth conditions that set demand to build and maintain photosynthetic enzymes than through changes in soil resource availability (Dong *et al.*, 2017, 2020, 2022a; Smith *et al.*, 2019; Smith & Keenan, 2020; Paillassa *et al.*, 2020; Peng *et al.*, 2021; Querejeta *et al.*, 2022; Westerband *et al.*, 2023; Waring *et al.*, 2023). These patterns indicate that leaf photosynthetic responses to elevated CO_2 may be a product of altered leaf nitrogen demand to build and maintain photosynthetic enzymes and may not be linked to changes in nitrogen availability.

Eco-evolutionary optimality theory provides a framework for understanding how leaf photosynthetic responses to elevated CO_2 may be determined through demand to build and maintain photosynthetic enzymes (Harrison *et al.*, 2021). Merging photosynthetic least-cost (Wright *et al.*, 2003; Prentice *et al.*, 2014) and optimal coordination (Chen *et al.*, 1993; Maire *et al.*, 2012) theories, eco-evolutionary optimality theory posits that reduced leaf nitrogen allocation under elevated CO_2 is the downstream result of a stronger downregulation in the maximum rate of Rubisco carboxylation (V_{cmax}) than the maximum rate of electron transport for RuBP regeneration (J_{max}), which reduces leaf nitrogen demand to build and maintain photosynthetic enzymes. Optimal leaf nitrogen allocation to photosynthetic capacity allows plants to make more efficient use of available light while avoiding overinvestment in Rubisco, which has high nitrogen and energetic costs of construction and maintenance (Evans, 1989; Sage, 1994; Evans & Clarke, 2019). Such optimal leaf nitrogen allocation responses to elevated CO_2 increases photosynthetic nitrogen-use efficiency and allows increased net photosynthesis rates to be achieved through increasingly equal co-limitation of Rubisco carboxylation and electron transport for RuBP regeneration (Chen *et al.*, 1993; Maire *et al.*, 2012; Wang *et al.*, 2017; Smith *et al.*, 2019). The expected optimal leaf response to elevated CO_2 has received some empirical support (Crous *et al.*, 2010; Lee *et al.*, 2011; Smith & Keenan, 2020; Harrison *et al.*, 2021; Dong *et al.*, 2022b; Cui *et al.*, 2023), though no studies have connected these patterns with concurrently measured whole-plant responses.

The eco-evolutionary optimality hypothesis deviates from the progressive nitrogen limitation hypothesis by indicating that photosynthetic responses to elevated CO_2 are driven by leaf nitrogen demand to build and maintain photosynthetic enzymes and are independent of soil nitrogen supply. However, the eco-evolutionary optimality hypothesis does not discount the role of soil nitrogen availability on modifying whole-plant responses to elevated CO_2, where the expected optimal strategy in response to elevated CO_2 is to allocate surplus nitrogen not needed to satisfy leaf nitrogen demand toward the construction of a greater quantity of optimally coordinated leaves and other plant organs. Thus, whether the supply-driven progressive nitrogen limitation hypothesis or demand-driven eco-evolutionary optimality hypothesis drives plant responses to elevated CO_2 may be a matter of scale, where leaf photosynthetic responses to elevated CO_2 are determined through demand to build and maintain photosynthetic enzymes and whole-plant responses to elevated CO_2 are regulated by changes in nitrogen supply.

Plants allocate carbon belowground in exchange for nutrients through different nutrient acquisition strategies, including direct uptake pathways or symbioses with mycorrhizal fungi or symbiotic nitrogen-fixing bacteria (Gutschick, 1981; Smith & Read, 2008). Carbon costs to acquire nitrogen, or the amount of carbon allocated belowground per unit nitrogen acquired, vary in species with different nitrogen acquisition strategies and are dependent on environmental factors such as atmospheric CO_2, temperature, light availability, and nutrient availability (Brzostek *et al.*, 2014; Terrer *et al.*, 2018; Allen *et al.*, 2020; Perkowski *et al.*, 2021; Peng *et al.*, 2023). Therefore, nitrogen acquisition strategy cannot be ignored when considering effects of nitrogen availability on plant responses to elevated CO_2. To date, few studies account for acquisition strategy when considering the role of nitrogen availability on leaf and whole-plant responses to elevated CO_2 (e.g., Terrer *et al.*, 2016, 2018; Smith & Keenan, 2020). Such studies found that nitrogen acquisition strategies with reduced carbon costs to acquire nitrogen may buffer the effect of nitrogen limitation at the whole-plant level (Terrer *et al.*, 2018), but leaf-level responses remain inconsistent (Terrer *et al.*, 2018; Smith & Keenan, 2020).

Here, we conducted a growth chamber experiment using *Glycine max* L. (Merr.) seedlings grown under full factorial combinations of two CO_2 concentrations, two inoculation treatments, and nine soil nitrogen fertilization treatments to reconcile the role of nitrogen supply and demand on plant responses to elevated CO_2. We used this experimental setup to test the following hypotheses:

155 (1) Following the demand-driven eco-evolutionary optimality hypothesis, elevated CO_2 will
156 downregulate V_{cmax} more strongly than J_{max}, increasing J_{max}:V_{cmax} and allowing increased
157 net photosynthesis rates to be achieved by approaching equal co-limitation of Rubisco
158 carboxylation and electron transport for RuBP regeneration. Leaf photosynthetic
159 responses to elevated CO_2 will be independent of nitrogen fertilization and inoculation
160 treatment and will correspond with increased photosynthetic nitrogen-use efficiency.
161 (2) Following the supply-driven nitrogen limitation hypothesis, positive effects of elevated
162 CO_2 on total leaf area and total biomass will be enhanced with increasing nitrogen
163 fertilization due to increased plant nitrogen uptake and corresponding reductions in
164 carbon costs to acquire nitrogen. Inoculation with symbiotic nitrogen-fixing bacteria will
165 enhance positive growth responses to elevated CO_2, though these responses will only be
166 apparent under low nitrogen fertilization levels where individuals will have increased
167 investment in nitrogen acquisition through symbiotic nitrogen fixation.
168

169 **Methods**

170 *Seed treatments and experimental design*

171 *Glycine max* seeds were planted in 144 6-liter surface sterilized pots (NS-600, Nursery Supplies,
172 Orange, CA, USA) containing a steam-sterilized 70:30 v:v mix of *Sphagnum* peat moss (Premier
173 Horticulture, Quakertown, PA, USA) to sand (Pavestone, Atlanta, GA, USA). Before planting,
174 all *G. max* seeds were surface sterilized in 2% sodium hypochlorite for 3 minutes, followed by
175 three separate 3-minute washes with ultrapure water (MilliQ 7000; MilliporeSigma, Burlington,
176 MA USA). Subsets of surface-sterilized seeds were inoculated with *Bradyrhizobium japonicum*
177 (Verdesian N-Dure™ Soybean, Cary, NC, USA) in a slurry following manufacturer
178 recommendations (3.12 g inoculant and 241 g ultrapure water per 1 kg seed).

179 Seventy-two pots were randomly planted with surface-sterilized seeds inoculated with *B.*
180 *japonicum*, while the remaining 72 pots were planted with surface-sterilized uninoculated seeds.
181 Thirty-six pots within each inoculation treatment were randomly placed in one of two
182 atmospheric CO_2 treatments (420 and 1000 μmol mol^{-1} CO_2). Plants in each unique inoculation-
183 by-CO_2 treatment combination randomly received one of nine nitrogen fertilization treatments
184 equivalent to 0 (0 mM), 35 (2.5 mM), 70 (5 mM), 105 (7.5 mM), 140 (10 mM), 210 (15 mM),
185 280 (20 mM), 350 (25 mM), or 630 ppm (45 mM) N. Nitrogen fertilization treatments were

created using a modified Hoagland's solution (Hoagland & Arnon, 1950) designed to keep concentrations of all other macronutrients and micronutrients equivalent across treatments (Table S1). Plants received the same nitrogen fertilization treatment twice per week in 150 mL doses as topical agents to the soil surface.

Growth chamber conditions

Plants were randomly placed in one of six Percival LED-41L2 growth chambers (Percival Scientific Inc., Perry, IA, USA) over two experimental iterations due to chamber space limitation. Two iterations were conducted such that one iteration included all plants grown under elevated CO_2 plants, and the second iteration included all plants grown under ambient CO_2. Average (± SD) CO_2 concentrations across chambers throughout the experiment were 439±5 μmol mol^{-1} for the ambient CO_2 treatment and 989±4 μmol mol^{-1} for the elevated CO_2 treatment.

Daytime growth conditions were simulated using a 16-hour photoperiod, with incoming light radiation set to chamber maximum (mean±SD: 1230±12 μmol m^{-2} s^{-1} across chambers), air temperature set to 25°C, and relative humidity set to 50%. The remaining 8-hour period simulated nighttime growing conditions, with incoming light radiation set to 0 μmol m^{-2} s^{-1}, chamber temperature set to 17°C, and relative humidity set to 50%. Transitions between daytime and nighttime growing conditions were simulated by ramping incoming light radiation in 45-minute increments and temperature in 90-minute increments over a 3-hour period (Table S2).

Plants grew under average (± SD) daytime light intensity of 1049±27 μmol m^{-2} s^{-1}, including ramping periods. In the elevated CO_2 iteration, plants grew under 24.0±0.2°C during the day, 16.4±0.8°C during the night, and 51.6±0.4% relative humidity. In the ambient CO_2 iteration, plants grew under 23.9±0.2°C during the day, 16.0±1.4°C during the night, and 50.3±0.2% relative humidity. Within each experiment iteration, any differences in climate conditions across the six chambers were accounted for by shuffling the same group of plants throughout the growth chambers. This process was done by iteratively moving the group of plants on the top rack of a chamber to the bottom rack of the same chamber, while simultaneously moving the group of plants on the bottom rack of a chamber to the top rack of the adjacent chamber. Plants were moved within and across chambers daily during each experiment iteration.

Leaf gas exchange measurements

Leaf gas exchange measurements were collected on the seventh week of development, before the onset of reproduction. All gas exchange measurements were collected on the center leaf of the most recent fully expanded trifoliate leaf set. Specifically, net photosynthesis (A_{net}; µmol m^{-2} s^{-1}), stomatal conductance (g_{sw}; mol m^{-2} s^{-1}), and intercellular CO_2 (C_i; µmol mol^{-1}) concentrations were measured across a range of atmospheric CO_2 concentrations (i.e., an A_{net}/C_i curve) using the Dynamic Assimilation™ Technique. The Dynamic Assimilation™ Technique corresponds well with traditional steady-state A_{net}/C_i curves in *G. max* (Saathoff & Welles, 2021). A_{net}/C_i curves were generated along a reference CO_2 ramp down from 420 µmol mol^{-1} CO_2 to 20 µmol mol^{-1} CO_2, followed by a ramp up from 420 µmol mol^{-1} CO_2 to 1620 µmol mol^{-1} CO_2 after a 90-second wait period at 420 µmol mol^{-1} CO_2. The ramp rate for each curve was set to 200 µmol mol^{-1} min^{-1}, logging every five seconds, which generated 96 data points per response curve. All A_{net}/C_i curves were generated after A_{net} and g_{sw} stabilized in a LI-6800 cuvette set to a 500 mol s^{-1} flow rate, 10000 rpm mixing fan speed, 1.5 kPa vapor pressure deficit, 25°C leaf temperature, 2000 µmol m^{-2} s^{-1} incoming light radiation, and initial reference CO_2 set to 420 µmol mol^{-1}.

Snapshot A_{net} measurements were extracted from each A_{net}/C_i curve, both at a common CO_2 concentration, 420 µmol mol^{-1} CO_2 ($A_{net,420}$; µmol m^{-2} s^{-1}), and under each individual's growth CO_2 concentration, 420 and 1000 µmol mol^{-1} CO_2 ($A_{net,growth}$; µmol m^{-2} s^{-1}). Dark respiration (R_d; µmol m^{-2} s^{-1}) measurements were collected with the same leaf used to generate A_{net}/C_i curves following at least 30 minutes of darkness. Measurements were collected on a 5-second log interval for 60 seconds after the leaf stabilized in a LI-6800 cuvette set to a 500 mol s^{-1} flow rate, 10000 rpm mixing fan speed, 1.5 kPa vapor pressure deficit, 25°C leaf temperature, and 420 µmol mol^{-1} reference CO_2 concentration (regardless of CO_2 treatment), with incoming light radiation set to 0 µmol m^{-2} s^{-1}. A single dark respiration value was determined for each leaf by calculating the mean dark respiration value across the logging interval.

A/C_i curve-fitting and parameter estimation

A_{net}/C_i curves were fit using the 'fitaci' function in the 'plantecophys' R package (Duursma, 2015). This function estimates the maximum rate of Rubisco carboxylation (V_{cmax}; µmol m^{-2} s^{-1}) and maximum rate of electron transport for RuBP regeneration (J_{max}; µmol m^{-2} s^{-1}) based on the Farquhar *et al.* (1980) biochemical model of C_3 photosynthesis. Triose phosphate utilization

248 (TPU) limitation was included as an additional rate-limiting step in all curve fits after visually
249 observing clear TPU limitation for most curves. All curve fits included measured dark respiration
250 values. As A_{net}/C_i curves were generated using a common leaf temperature (25°C), curves were
251 fit using Michaelis-Menten coefficients for Rubisco affinity to CO_2 (K_c; μmol mol^{-1}) and O_2 (K_o;
252 mmol mol^{-1}), and the CO_2 compensation point (Γ^*; μmol mol^{-1}) reported in Bernacchi *et al.*
253 (2001). Specifically, K_c was set to 404.9 μmol mol^{-1}, K_o was set to 278.4 μmol mol^{-1}, and Γ^* was
254 set to 42.75 μmol mol^{-1}. For clarity, V_{cmax}, J_{max}, and R_d estimates are referenced throughout the
255 rest of the paper as V_{cmax25}, J_{max25}, and R_{d25}.
256
257 *Leaf trait measurements*
258 The leaf used to generate A_{net}/C_i curves and dark respiration measurements was harvested
259 immediately following gas exchange measurements. Images of each focal leaf were curated
260 using a flat-bed scanner to determine fresh leaf area using the 'LeafArea' R package (Katabuchi,
261 2015), which automates leaf area calculations using ImageJ software (Schneider *et al.*, 2012).
262 Post-processed images were visually assessed to check against errors in the automation process.
263 Each leaf was dried at 65°C for at least 48 hours and subsequently weighed and ground until
264 homogenized. Leaf mass per area (M_{area}; g m^{-2}) was calculated as the ratio of dry leaf biomass to
265 fresh leaf area. Leaf nitrogen content (N_{mass}; gN g^{-1}) was quantified using a subsample of ground
266 and homogenized leaf tissue through elemental combustion analysis (Costech-4010, Costech,
267 Inc., Valencia, CA, USA). Leaf nitrogen content per unit leaf area (N_{area}; gN m^{-2}) was calculated
268 by multiplying N_{mass} and M_{area}. Photosynthetic nitrogen-use efficiency ($PNUE_{growth}$; μmol CO_2
269 g^{-1} N s^{-1}) was estimated as the ratio of $A_{net,growth}$ to N_{area}.
270 Chlorophyll content was extracted from a second leaf in the same trifoliate leaf set as the
271 leaf used to generate A_{net}/C_i curves. A cork borer was used to punch between 3-5 0.6 cm^2 disks
272 from the leaf. Images of each set of leaf disks were curated using a flat-bed scanner to determine
273 wet leaf area, again quantified using the 'LeafArea' R package (Katabuchi, 2015). Leaf disks
274 were shuttled into a test tube containing 10 mL dimethyl sulfoxide, vortexed, and incubated at
275 65°C for 120 minutes (Barnes *et al.*, 1992). Incubated test tubes were vortexed again before
276 being loaded in 150 μL triplicate aliquots to a 96-well plate. Dimethyl sulfoxide was loaded in
277 each plate as a single 150 μL triplicate aliquot and used as a blank. Absorbance measurements at
278 649 nm (A_{649}) and 665 nm (A_{665}) were recorded in each well using a plate reader (Biotek Synergy

H1; Biotek Instruments, Winooski, VT USA), with triplicates averaged and corrected by the mean of the blank absorbance value. Blank-corrected absorbance values were used to estimate Chl_a (μg mL^{-1}) and Chl_b (μg mL^{-1}) following equations from Wellburn (1994):

$$Chl_a = 12.47A_{665} - 3.62A_{649} \quad (1)$$

and

$$Chl_b = 25.06A_{649} - 6.5A_{665} \quad (2)$$

Chl_a and Chl_b were converted to mmol mL^{-1} using the molar mass of chlorophyll *a* (893.51 g mol^{-1}) and the molar mass of chlorophyll *b* (907.47 g mol^{-1}), then added together to calculate the total chlorophyll content in dimethyl sulfoxide extractant (mmol mL^{-1}). Total chlorophyll content (mmol) was determined by multiplying the total chlorophyll content in dimethyl sulfoxide by the volume of dimethyl sulfoxide extractant (10 mL). Area-based chlorophyll content (Chl_{area}; mmol m^{-2}) was then calculated by dividing the total chlorophyll content by the total area of the leaf disks.

Subsamples of ground and homogenized leaf tissue were sent to the University of California-Davis Stable Isotope Facility to determine leaf $\delta^{13}C$ and $\delta^{15}N$ using an elemental analyzer (Elementar vario MICRO cube elemental analyzer; Elementar Analysensysteme GmbH, Langenselbold, Germany) interfaced to an isotope ratio mass spectrometer (PDZ Europa 20-20 Isotope Ratio Mass Spectrometer, Sercon Ltd., Chestshire, UK). Leaf $\delta^{13}C$ was used to estimate the time-integrated ratio of leaf intercellular CO_2 concentration to atmospheric CO_2 concentration (χ, unitless) using leaf $\delta^{13}C$ and chamber air $\delta^{13}C$ following equations from Farquhar *et al.* (1989):

$$\chi = \frac{\Delta^{13}C - a}{b - a} \quad (3)$$

where $\Delta^{13}C$ represents the relative difference between leaf $\delta^{13}C$ (‰) and air $\delta^{13}C$ (‰), and is calculated as:

$$\Delta^{13}C = \frac{\delta^{13}C_{air} - \delta^{13}C_{leaf}}{1 + \delta^{13}C_{leaf}} \quad (4)$$

$\delta^{13}C_{air}$ is the chamber $\delta^{13}C$ air fractionation, *a* represents the fractionation between ^{12}C and ^{13}C due to diffusion in air, assumed to be 4.4‰, and *b* represents the fractionation caused by Rubisco carboxylation, assumed to be 27‰ (Farquhar *et al.*, 1989). $\delta^{13}C_{air}$ was quantified in each chamber by collecting air samples in triplicate for each CO_2 treatment using a 20 mL syringe (Air-Tite Products Co., Inc., Virginia Beach, VA, USA). Each air sample was plunged into a

309 manually evacuated 10 mL Exetainer (Labco Ltd., Lampeter, UK) and sent to the University of
310 California-Davis Stable Isotope Facility, where $\delta^{13}C_{air}$ was determined using a gas inlet system
311 (GasBenchII; Thermo Fisher Scientific, Waltham, MA, USA) coupled to an isotope ratio mass
312 spectrometer (Thermo Finnigan Delta Plus XL; Thermo Fisher Scientific, Waltham, MA, USA).
313 $\delta^{13}C_{air}$ for each CO_2 treatment was estimated by calculating the mean of the triplicate $\delta^{13}C_{air}$
314 samples within each chamber, then calculating the mean $\delta^{13}C_{air}$ across all chambers. Specifically,
315 $\delta^{13}C_{air}$ was -8.81‰ for the ambient CO_2 treatment and -5.95‰ for the elevated CO_2 treatment.
316 Finally, the percent of leaf nitrogen acquired from the atmosphere (%N_{dfa}; %) was
317 estimated using leaf $\delta^{15}N$ and the following equation adapted from Andrews *et al.* (2011):

318 $$\% N_{dfa} = \frac{\delta^{15}N_{direct} - \delta^{15}N_{sample}}{\delta^{15}N_{direct} - \delta^{15}N_{fixation}} \quad (5)$$

319 where $\delta^{15}N_{direct}$ refers to the $\delta^{15}N$ value from plants that exclusively acquired nitrogen via direct
320 uptake, $\delta^{15}N_{sample}$ refers to an individual's leaf $\delta^{15}N$, and $\delta^{15}N_{fixation}$ refers to the $\delta^{15}N$ value from
321 individuals that were entirely reliant on nitrogen fixation. $\delta^{15}N_{direct}$ was calculated as the mean
322 leaf $\delta^{15}N$ of uninoculated individuals within each unique nitrogen fertilization-by-CO_2 treatment
323 combination. Any individual with visual evidence of root nodule formation or nodule initiation
324 was omitted from the calculation of $\delta^{15}N_{direct}$. $\delta^{15}N_{fixation}$ was calculated within each CO_2
325 treatment using the mean leaf $\delta^{15}N$ of inoculated individuals that received 0 ppm N. $\delta^{15}N_{fixation}$
326 was not calculated within each unique nitrogen fertilization-by-CO_2 treatment combination, as
327 previous studies suggest decreased reliance on nitrogen fixation with increasing nitrogen
328 fertilization (Perkowski *et al.*, 2021).
329
330 *Whole-plant measurements*
331 Seven weeks after experiment initiation and immediately following gas exchange measurements,
332 all individuals were harvested, and biomass of major organ types (leaves, stems, roots, and
333 nodules when present) were separated. Fresh leaf area of all harvested leaves was measured
334 using a LI-3100C (Li-COR Biosciences, Lincoln, Nebraska, USA). Total fresh leaf area (cm^2)
335 was calculated as the sum of all leaf areas, including the leaf used to collect gas exchange data
336 and the leaf used to extract chlorophyll content. All harvested material was dried in an oven set
337 to 65°C for at least 48 hours to a constant mass, weighed, and ground to homogeneity. Leaves
338 and nodules were ground using a mortar and pestle, while stems and roots were ground using an

339 E3300 Single Speed Mini Cutting Mill (Eberbach Corp., MI, USA). Total biomass (g) was
340 calculated as the sum of dry leaf, stem, root, and root nodule biomass. Carbon and nitrogen
341 content was measured for each organ type through elemental combustion (Costech-4010,
342 Costech, Inc., Valencia, CA, USA) using subsamples of ground and homogenized organ tissue.
343 The ratio of root nodule biomass to root biomass was calculated as an additional indicator of
344 investment toward symbiotic nitrogen fixation.
345 Following Perkowski *et al.* (2021), carbon costs to acquire nitrogen were quantified as
346 the ratio of belowground carbon biomass to total nitrogen biomass (N_{cost}; gC gN^{-1}). Belowground
347 carbon biomass (C_{bg}; gC) was calculated as the sum of root carbon biomass and root nodule
348 carbon biomass. Root carbon biomass and root nodule carbon biomass were calculated as the
349 product of the organ biomass and respective organ carbon content. Total nitrogen biomass (N_{wp};
350 gN) was calculated as the sum of total leaf, stem, root, and root nodule nitrogen biomass. Leaf,
351 stem, root, and root nodule nitrogen biomass was calculated as the product of the organ biomass
352 and respective organ nitrogen content. This calculation does not account for additional carbon
353 costs to acquire nitrogen associated with respiration, root exudation, or root turnover, and
354 therefore may underestimate carbon costs to acquire nitrogen (Perkowski *et al.*, 2021).
355
356 *Statistical analyses*
357 Uninoculated plants that had substantial root nodule formation (nodule biomass: root biomass
358 values greater than 0.05 g g^{-1}) were removed from analyses under the assumption that plants
359 were either incompletely sterilized or were colonized by symbiotic nitrogen-fixing bacteria from
360 neighboring plants in the chamber. This decision resulted in the removal of sixteen plants from
361 the analysis: two plants in the elevated CO_2 treatment that received 35 ppm N, three plants in the
362 elevated CO_2 treatment that received 70 ppm N, one plant in the elevated CO_2 treatment that
363 received 210 ppm N, two plants in the elevated CO_2 treatment that received 280 ppm N, two
364 plants in the ambient CO_2 treatment that received 0 ppm N, three plants in the ambient CO_2
365 treatment that received 70 ppm N, two plants in the ambient CO_2 treatment that received 105
366 ppm N, and one plant in the ambient CO_2 treatment that received 280 ppm N.
367 A series of linear mixed-effects models were built to investigate the impacts of CO_2
368 concentration, nitrogen fertilization, and inoculation on *G. max* leaf nitrogen allocation, gas
369 exchange, whole-plant growth, and investment in nitrogen fixation. All models included CO_2

treatment as a categorical fixed effect, inoculation treatment as a categorical fixed effect, and nitrogen fertilization as a continuous fixed effect, with all possible interaction terms between all three fixed effects also included. Models accounted for climatic differences between chambers across experiment iterations by including a random intercept term that nested the starting chamber rack by CO_2 treatment. Models with this independent variable structure were created for each of the following dependent variables: N_{area}, M_{area}, N_{mass}, Chl_{area}, $A_{net,420}$, $A_{net,growth}$, R_{d25}, V_{cmax25}, J_{max25}, J_{max25}:V_{cmax25}, $PNUE_{growth}$, χ, N_{cost}, C_{bg}, N_{wp}, total biomass, total leaf area, $\%N_{dfa}$, root nodule biomass, root nodule biomass: root biomass, and the ratio of total biomass to potting volume.

Shapiro-Wilk tests of normality were used to assess whether linear mixed-effects models satisfied residual normality assumptions. All models that did not satisfy residual normality assumptions satisfied such assumptions when response variables were fit using either a natural log or square root data transformation (Shapiro-Wilk: $p>0.05$ in all cases). Specifically, models for N_{area}, N_{mass}, Chl_{area}, $A_{net,420}$, $A_{net,growth}$, R_{d25}, V_{cmax25}, J_{max25}, J_{max25}:V_{cmax25}, $PNUE_{growth}$, χ, total leaf area, N_{cost}, and the ratio of total biomass to pot volume each satisfied residual normality assumptions without data transformation. Models for M_{area}, total biomass, and C_{bg} satisfied residual normality assumptions with a natural log data transformation, while models for N_{wp}, nodule biomass, nodule biomass: root biomass, and $\%N_{dfa}$ satisfied residual normality assumptions with a square root data transformation.

In all models, we used the ‘lmer’ function in the ‘lme4’ R package (Bates *et al.*, 2015) to fit each model and the ‘Anova’ function in the ‘car’ R package (Fox & Weisberg, 2019) to calculate Type II Wald's χ^2 and determine the significance (α=0.05) of each fixed effect coefficient. We used the ‘emmeans’ R package (Lenth, 2019) to conduct post-hoc comparisons using Tukey's tests, where degrees of freedom were approximated using the Kenward-Roger approach (Kenward & Roger, 1997). Trendlines and error ribbons representing the 95% confidence intervals were drawn in all figures using ‘emmeans’ outputs across the range in nitrogen fertilization values. All analyses and plots were conducted in R version 4.1.0 (R Core Team, 2021). Model results for χ, C_{bg}, N_{wp}, root nodule biomass, root nodule biomass: root biomass, and the ratio of total biomass to pot volume are reported in the *Supplemental Material* (Tables S3-S6; Figs. S3-S6).

401 **Results**

402 *Leaf nitrogen content*

403 Elevated CO_2 reduced N_{area}, N_{mass}, and Chl_{area} by 29%, 50%, and 31%, respectively, and
404 increased M_{area} by 44% ($p<0.001$ in all cases; Table 1). Interactions between nitrogen
405 fertilization and CO_2 ($p<0.05$ in all cases; Table 1) indicated that positive effects of increasing
406 nitrogen fertilization on N_{area}, N_{mass}, and M_{area} ($p<0.001$ in all cases; Table 1) were stronger under
407 ambient CO_2 than elevated CO_2 (Tukey test of the nitrogen fertilization-trait slope between CO_2:
408 $p<0.05$ in all cases). These responses resulted in a stronger reduction in N_{area} and N_{mass} and a
409 stronger increase in M_{area} under elevated CO_2 with increasing nitrogen fertilization than ambient
410 CO_2 (Fig. S1). Nitrogen fertilization did not modify reductions in Chl_{area} due to elevated CO_2
411 (Tukey test of the nitrogen fertilization-Chl_{area} slope between CO_2 treatments: $p>0.05$).

412 An interaction between inoculation and CO_2 ($p<0.05$; Table 1) indicated that reductions
413 in N_{area} due to elevated CO_2 were stronger in uninoculated plants. Specifically, uninoculated
414 plants experienced a 36% reduction in N_{area} (Tukey test of the CO_2 effect in uninoculated plants:
415 $p<0.001$), while inoculated plants experienced a 22% reduction (Tukey test of the CO_2 effect in
416 inoculated plants: $p<0.001$). Inoculation did not modify N_{mass}, M_{area}, or Chl_{area} responses to
417 elevated CO_2 (CO_2-by-inoculation interaction: $p>0.05$ in all cases; Table 1). However, an
418 interaction between nitrogen fertilization and inoculation ($p<0.05$ in all cases; Table 1; Figs. 1a-
419 d) indicated that positive effects of increasing nitrogen fertilization on N_{area}, N_{mass}, M_{area}, and
420 Chl_{area} ($p<0.001$ in all cases; Table 1) were stronger in uninoculated plants compared to
421 inoculated plants (Tukey test of the nitrogen fertilization-trait slope between inoculation
422 treatments: $p<0.05$ in all cases).

423

Table 1 Effects of nitrogen fertilization, inoculation, and CO_2 treatments on leaf nitrogen allocation*

		N_{area}		N_{mass}		M_{area}[a]		Chl_{area}	
	df	χ^2	*p*	χ^2	*p*	χ^2	*p*	χ^2	*p*
CO_2	1	155.908	**<0.001**	272.362	**<0.001**	151.319	**<0.001**	69.233	**<0.001**
Inoculation (I)	1	86.029	**<0.001**	15.576	**<0.001**	19.158	**<0.001**	136.341	**<0.001**
N fertilization (N)	1	316.408	**<0.001**	106.659	**<0.001**	21.440	**<0.001**	163.111	**<0.001**
CO_2*I	1	4.729	**0.030**	2.025	0.155	0.029	0.866	2.102	0.147
CO_2*N	1	5.723	**0.017**	22.542	**<0.001**	7.619	**0.006**	2.999	0.083
I*N	1	43.381	**<0.001**	11.137	**0.001**	5.022	**0.025**	75.769	**<0.001**
CO_2*I*N	1	0.489	0.484	0.041	0.839	0.208	0.649	2.144	0.143

*Significance determined using Type II Wald χ^2 tests (α=0.05). *P*-values less than 0.05 are in bold. A superscript "a" is included after trait labels to indicate if models were fit with natural log transformed response variables. Key: df=degrees of freedom, χ^2=Wald chi-square test statistic, N_{area}=leaf nitrogen content per unit leaf area (gN m^{-2}), N_{mass}=leaf nitrogen content (gN g^{-1}), M_{area}=leaf mass per unit leaf area (g m^{-2}).

Figure 1

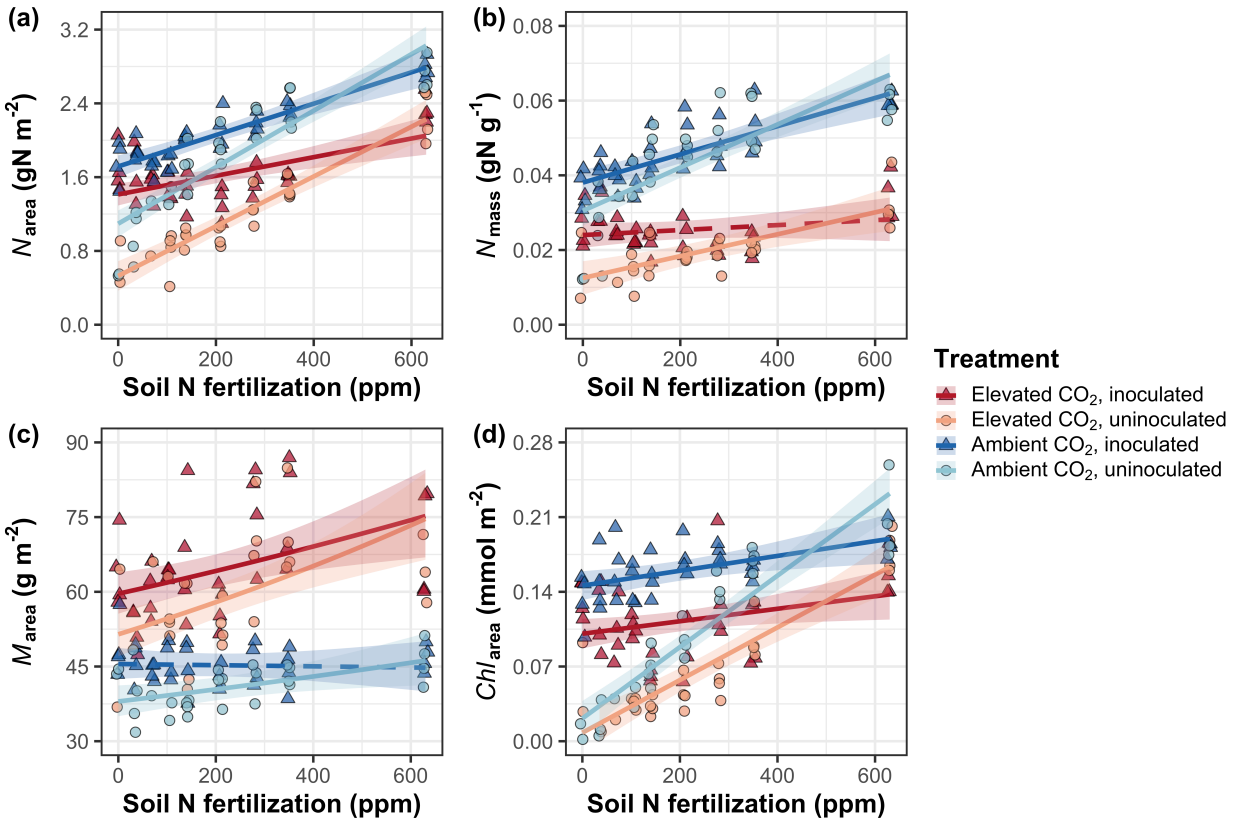

Figure 1 Effects of CO_2 concentration, nitrogen fertilization, and inoculation on leaf nitrogen per unit leaf area (a), leaf nitrogen per unit leaf mass (b), leaf mass per unit leaf area (c), and chlorophyll content per unit leaf area (d). Nitrogen fertilization is represented on the x-axis in all panels. Red shaded points and trendlines indicate plants grown under elevated CO_2, while blue shaded points and trendlines indicate plants grown under ambient CO_2. Light blue and red circular points and trendlines indicate measurements collected from uninoculated plants, while dark blue and red triangular points indicate measurements collected from inoculated plants. Solid trendlines indicate regression slopes that are different from zero (p<0.05), while dashed trendlines indicate slopes that are not distinguishable from zero (p>0.05).

442 *Gas exchange*

443 Elevated CO_2 decreased $A_{net,420}$ by 17% (p<0.001; Table 2) and increased $A_{net,growth}$ by 33%
444 (p<0.001; Table 2). Nitrogen fertilization did not modify effects of elevated CO_2 on $A_{net,420}$ or
445 $A_{net,growth}$ (CO_2-by-nitrogen fertilization interaction: p>0.05 in both cases; Table 2; Fig. 2a-b).
446 Inoculation did not modify the negative effect of elevated CO_2 on $A_{net,420}$ (CO_2-by-inoculation
447 interaction: p>0.05); however, an interaction between CO_2 and inoculation (p<0.05; Table 2)
448 indicated that inoculated plants experienced a stronger increase in $A_{net,growth}$ under elevated CO_2
449 than uninoculated plants. Specifically, inoculated plants experienced a 38% increase in $A_{net,growth}$
450 under elevated CO_2 (Tukey test of the CO_2 effect in inoculated plants: p<0.001), while
451 uninoculated plants experienced a 26% increase (Tukey test of the CO_2 effect in uninoculated
452 plants: p<0.05). An interaction between nitrogen fertilization and inoculation (p<0.001 in both
453 cases; Table 2) indicated that positive effects of increasing nitrogen fertilization on $A_{net,420}$ and
454 $A_{net,growth}$ (p<0.001 in both cases; Table 2; Fig. 2a-b) were stronger in uninoculated plants than
455 inoculated plants (Tukey test comparing the nitrogen fertilization-trait slope between inoculation
456 treatments: p<0.001 in both cases).

457 Elevated CO_2 decreased V_{cmax25} and J_{max25} by 16% and 10%, respectively, increasing
458 J_{max25}:V_{cmax25} by 8% (p<0.05 in all cases; Table 2; Figs. 2c-e). V_{cmax25}, J_{max25}, and J_{max25}:V_{cmax25}
459 responses to elevated CO_2 were not modified by nitrogen fertilization (CO_2-by-nitrogen
460 fertilization interaction: p>0.05 in all cases; Table 2; Fig. 2c-e) or inoculation (CO_2-by-
461 inoculation interaction: p>0.05 in all cases; Table 2). An interaction between nitrogen
462 fertilization and inoculation (p<0.05 in both cases; Table 2) indicated that positive effects of
463 increasing nitrogen fertilization on V_{cmax25} and J_{max25} (p<0.001 in both cases; Table 2) and
464 negative effects of increasing nitrogen fertilization on J_{max25}:V_{cmax25} (p<0.001; Table 2) were
465 driven by uninoculated plants (Tukey test of the nitrogen fertilization-trait slope in uninoculated
466 plants: p<0.001 in all cases), as there was no effect of nitrogen fertilization on V_{cmax25}, J_{max25}, or
467 J_{max25}:V_{cmax25} in inoculated plants (Tukey test of the nitrogen fertilization-trait slope in inoculated
468 plants: p>0.05 in all cases).

469 There was no effect of CO_2 concentration on R_{d25} (p>0.05; Table 2). An interaction
470 between nitrogen fertilization and inoculation (p<0.001; Table 2) indicated that the positive
471 effect of increasing nitrogen fertilization on R_{d25} (p=0.015; Table 2) was driven by uninoculated
472 plants (Tukey test of the nitrogen fertilization-R_{d25} slope in uninoculated plants: p<0.001), as

473 there was no effect of nitrogen fertilization on R_{d25} in inoculated plants (Tukey test of the
474 nitrogen fertilization-R_{d25} slope in inoculated plants: $p>0.05$).
475

Table 2 Effects of nitrogen fertilization, inoculation, and CO_2 on leaf gas exchange and photosynthetic nitrogen-use efficiency*

		$A_{net,420}$		$A_{net,growth}$		V_{cmax25}		J_{max25}	
	df	χ^2	*p*	χ^2	*p*	χ^2	*p*	χ^2	*p*
CO_2	1	15.747	**<0.001**	52.716	**<0.001**	18.039	**<0.001**	6.042	**0.014**
Inoculation (I)	1	77.137	**<0.001**	83.008	**<0.001**	98.579	**<0.001**	85.064	**<0.001**
N fertilization (N)	1	11.986	**<0.001**	14.658	**<0.001**	37.053	**<0.001**	25.356	**<0.001**
CO_2*I	1	1.032	0.310	5.634	**0.018**	0.065	0.799	0.667	0.414
CO_2*N	1	1.998	0.158	0.135	0.713	1.758	0.185	0.742	0.389
I*N	1	46.800	**<0.001**	50.774	**<0.001**	60.394	**<0.001**	57.41	**<0.001**
CO_2*I*N	1	0.002	0.964	1.332	0.248	0.748	0.387	0.377	0.539

		J_{max25}:V_{cmax25}		R_{d25}		$PNUE_{growth}$	
		χ^2	*p*	χ^2	*p*	χ^2	*p*
CO_2	1	92.010	**<0.001**	0.256	0.613	300.197	**<0.001**
Inoculation (I)	1	27.768	**<0.001**	3.094	0.079	9.897	**0.002**
N fertilization (N)	1	28.147	**<0.001**	5.965	**0.015**	29.695	**<0.001**
CO_2*I	1	2.916	0.088	2.563	0.109	0.944	0.331
CO_2*N	1	3.210	0.073	2.675	0.102	5.359	**0.021**
I*N	1	9.607	**0.002**	12.083	**0.001**	10.883	**<0.001**
CO_2*I*N	1	1.102	0.294	0.244	0.622	0.369	0.544

*Significance determined using Type II Wald χ^2 tests (α=0.05). *P*-values less than 0.05 are in bold. Key: df=degrees of freedom, χ^2=Wald chi-square test statistic, A_{net}=net photosynthesis rate (μmol m^{-2} s^{-1}), V_{cmax25}=maximum rate of Rubisco carboxylation at 25°C (μmol m^{-2} s^{-1}), J_{max25}=maximum rate of electron transport for RuBP regeneration at 25°C (μmol m^{-2} s^{-1}), J_{max25}:V_{cmax25}=ratio of J_{max25} to V_{cmax25} (unitless), R_{d25}=dark respiration at 25°C (μmol m^{-2} s^{-1}), $PNUE_{growth}$=photosynthetic nitrogen-use efficiency (μmol CO_2 gN^{-1} s^{-1})

483 **Figure 2**

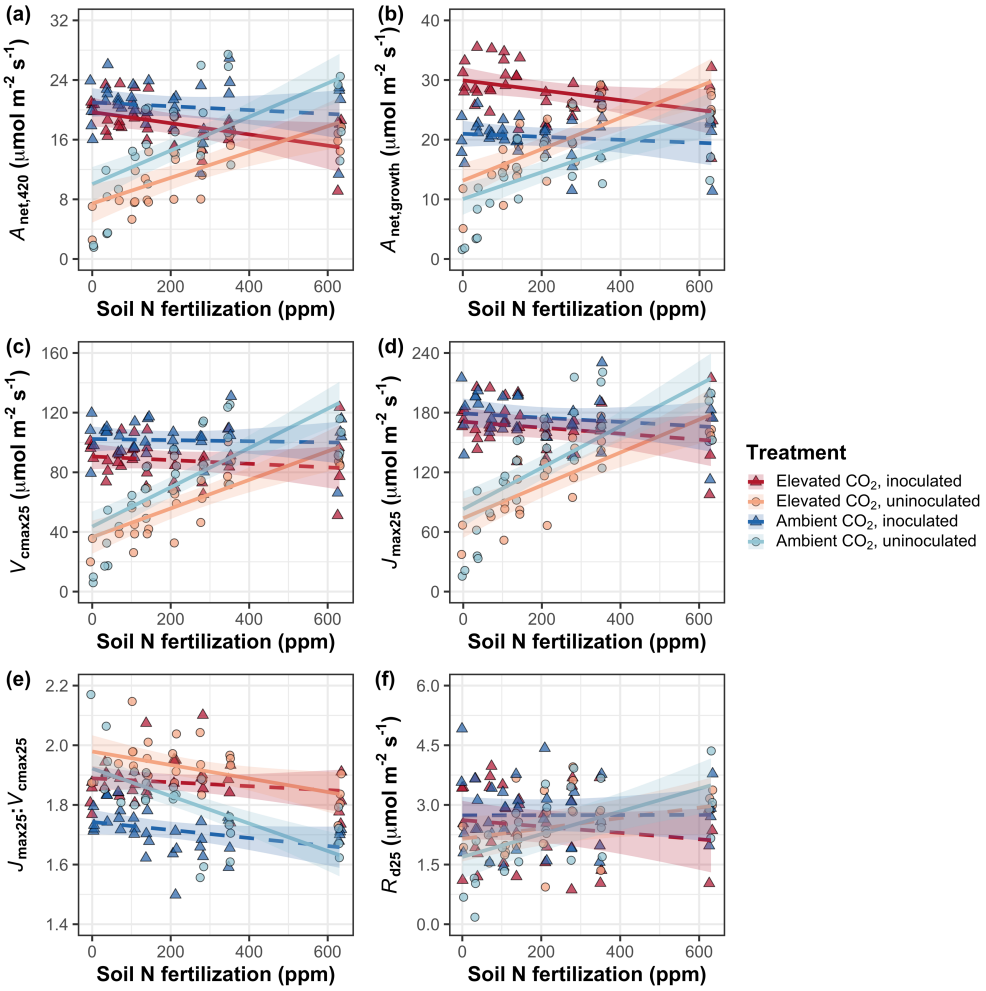

484

485 **Figure 2** Effects of CO_2, nitrogen fertilization, and inoculation on net photosynthesis measured
486 at 420 μmol mol^{-1} CO_2 (a), net photosynthesis measured under growth CO_2 concentration (b), the
487 maximum rate of Rubisco carboxylation at 25°C (c), the maximum rate of electron transport for
488 RuBP regeneration at 25°C (d), the ratio of the maximum rate of electron transport for RuBP
489 regeneration to the maximum rate of Rubisco carboxylation (e), and dark respiration at 25°C (f).
490 Nitrogen fertilization is represented on the x-axis. Red shaded points and trendlines indicate
491 plants grown under elevated CO_2, while blue shaded points and trendlines indicate plants grown
492 under ambient CO_2. Light blue and red circular points and trendlines indicate measurements
493 collected from uninoculated plants, while dark blue and red triangular points indicate
494 measurements collected from inoculated plants. Solid trendlines indicate regression slopes that
495 are different from zero (p<0.05), while dashed trendlines indicate slopes that are not
496 distinguishable from zero (p>0.05)

497 *Photosynthetic nitrogen-use efficiency*

498 Elevated CO_2 increased $PNUE_{growth}$ by 90% ($p<0.001$; Table 2; Fig. 3), a pattern that was not
499 modified by inoculation treatment (CO_2-by-inoculation interaction: $p>0.05$; Table 2). An
500 interaction between CO_2 and nitrogen fertilization ($p=0.021$; Table 2) indicated that the positive
501 effect of elevated CO_2 on $PNUE_{growth}$ decreased with increasing nitrogen fertilization (Fig. S2).
502 This pattern was driven by a negative effect of increasing nitrogen fertilization on $PNUE_{growth}$
503 ($p<0.001$; Table 2) that was stronger under elevated CO_2 compared to ambient CO_2 (Tukey test
504 comparing the nitrogen fertilization-$PNUE_{growth}$ slope between CO_2 treatments: $p<0.05$). An
505 interaction between nitrogen fertilization and inoculation ($p<0.001$; Table 2; Fig. 3) indicated
506 that the negative effect of increasing nitrogen fertilization on $PNUE_{growth}$ was driven by
507 inoculated plants (Tukey test of the nitrogen fertilization-$PNUE_{growth}$ slope in inoculated plants:
508 $p<0.001$), as there was no effect of nitrogen fertilization on $PNUE_{growth}$ in uninoculated plants
509 (Tukey test of the nitrogen fertilization-$PNUE_{growth}$ slope in uninoculated plants: $p>0.05$).
510

Figure 3

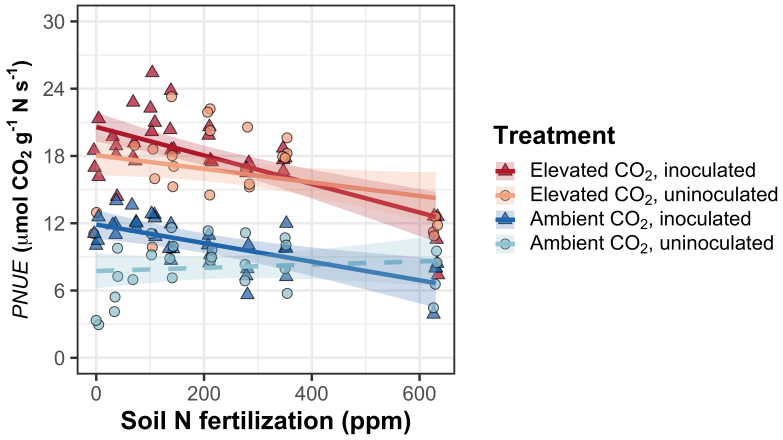

Figure 3 Effects of CO_2, nitrogen fertilization, and inoculation on photosynthetic nitrogen-use efficiency. Nitrogen fertilization is represented on the x-axis. Red shaded points and trendlines indicate plants grown under elevated CO_2, while blue shaded points and trendlines indicate plants grown under ambient CO_2. Light blue and red circular points and trendlines indicate measurements collected from uninoculated plants, while dark blue and red triangular points indicate measurements collected from inoculated plants. Solid trendlines indicate regression slopes that are different from zero ($p<0.05$), while dashed trendlines indicate slopes that are not distinguishable from zero ($p>0.05$).

522 *Whole-plant traits*

523 Elevated CO_2 increased total leaf area and total biomass by 51% and 102%, respectively
524 (p<0.001 in both cases; Table 3). Positive effects of elevated CO_2 on total leaf area and total
525 biomass were enhanced with increasing nitrogen fertilization (CO_2-by-nitrogen fertilization
526 interaction: p<0.001 in both cases; Table 3; Fig. 4a-b) but not inoculation (CO_2-by-inoculation
527 interaction: p>0.05 in both cases; Table 3). An interaction between nitrogen fertilization and
528 inoculation (p<0.001 in both cases; Table 3) indicated that positive effects of increasing nitrogen
529 fertilization on total leaf area and total biomass (p<0.001 in both cases; Table 3) were stronger in
530 uninoculated plants than inoculated plants (Tukey tests comparing the nitrogen fertilization-trait
531 slopes between inoculation treatments: p<0.05 for both traits).

532 Elevated CO_2 increased N_{cost} by 62% (p<0.001; Table 3), a pattern that was not modified
533 by nitrogen fertilization (CO_2-by-nitrogen fertilization interaction: p>0.05; Table 3). An
534 interaction between CO_2 and inoculation (p<0.05; Table 3) indicated that the positive effect of
535 elevated CO_2 on N_{cost} was stronger in uninoculated plants. Specifically, elevated CO_2 increased
536 N_{cost} in uninoculated plants by 99% (Tukey test evaluating the CO_2 effect on N_{cost} in uninoculated
537 plants: p<0.001), but only by 21% in inoculated plants (Tukey test evaluating the CO_2 effect on
538 N_{cost} in inoculated plants: p<0.05). An interaction between nitrogen fertilization and inoculation
539 (p<0.001; Table 3) indicated that the negative effect of increasing nitrogen fertilization on N_{cost}
540 (p<0.001; Table 3) was stronger in uninoculated plants (Tukey test comparing the nitrogen
541 fertilization-N_{cost} slope between inoculation treatments: p<0.001). A three-way interaction
542 (p<0.001; Table 3) indicated that interactions between nitrogen fertilization and inoculation were
543 stronger under elevated CO_2 than ambient CO_2. This pattern was driven by greater N_{cost} in
544 uninoculated plants grown under elevated CO_2 and low nitrogen fertilization than any other CO_2-
545 by-inoculation treatment combination under soil low nitrogen fertilization (Tukey test comparing
546 N_{cost} in uninoculated individuals grown under elevated CO_2 and 0 ppm N to all other unique
547 CO_2-inoculation treatments grown under 0 ppm N: p<0.001 in all cases; Fig. 4c). N_{cost} was also
548 generally reduced in inoculated plants (p<0.001; Table 3). Negative effects of increasing
549 nitrogen fertilization and inoculation on N_{cost} were driven by stronger positive effects of each
550 treatment on N_{wp} than C_{bg}, while positive effects of elevated CO_2 on N_{cost} were driven by
551 stronger positive effects on C_{bg} than N_{wp} (Table S4; Fig. S4).

552

553 *Nitrogen fixation*

554 Elevated CO_2 had no effect on $\%N_{dfa}$ (p=0.472; Table 3). An interaction between nitrogen
555 fertilization and inoculation (p<0.001; Table 3) indicated that the negative effect of increasing
556 nitrogen fertilization on $\%N_{dfa}$ (p<0.001; Table 3) was driven by inoculated plants (Tukey test of
557 the nitrogen fertilization-$\%N_{dfa}$ slope in inoculated plants: p<0.001), as there was no effect of
558 nitrogen fertilization on $\%N_{dfa}$ in uninoculated plants (Tukey test of the nitrogen fertilization-
559 $\%N_{dfa}$ slope in uninoculated plants: p>0.05; Fig. 4d).

560

561 **Table 4** Effects of nitrogen fertilization, inoculation, and CO_2 on whole-plant growth, carbon costs to acquire nitrogen, and investment
562 in nitrogen fixation*

		Total leaf area		**Total biomass**[b]		**Carbon cost to acquire nitrogen**		**%N_{dfa}**[b]	
	df	χ^2	*p*	χ^2	*p*	χ^2	*p*	χ^2	*p*
CO_2	1	69.291	**<0.001**	131.477	**<0.001**	88.189	**<0.001**	0.518	0.472
Inoculation (I)	1	35.715	**<0.001**	34.264	**<0.001**	136.343	**<0.001**	955.57	**<0.001**
N fertilization (N)	1	274.199	**<0.001**	269.046	**<0.001**	80.501	**<0.001**	292.938	**<0.001**
CO_2*I	1	2.064	0.151	0.518	0.472	85.237	**<0.001**	2.010	0.156
CO_2*N	1	18.655	**<0.001**	16.877	**<0.001**	1.050	0.306	2.716	*0.099*
I*N	1	10.804	**0.001**	15.779	**<0.001**	46.489	**<0.001**	231.29	**<0.001**
CO_2*I*N	1	<0.001	0.990	0.023	0.880	18.125	**<0.001**	2.119	0.145

563 *Significance determined using Type II Wald χ^2 tests (α=0.05). *P*-values less than 0.05 are in bold and *p*-values between 0.05 and 0.10
564 are italicized. A superscript "b" after trait labels indicates if models were fit using square root transformed variables. Key: df=degrees
565 of freedom, χ^2=Wald chi-square test statistic, %N_{dfa}=percent nitrogen fixed from the atmosphere.

Figure 4

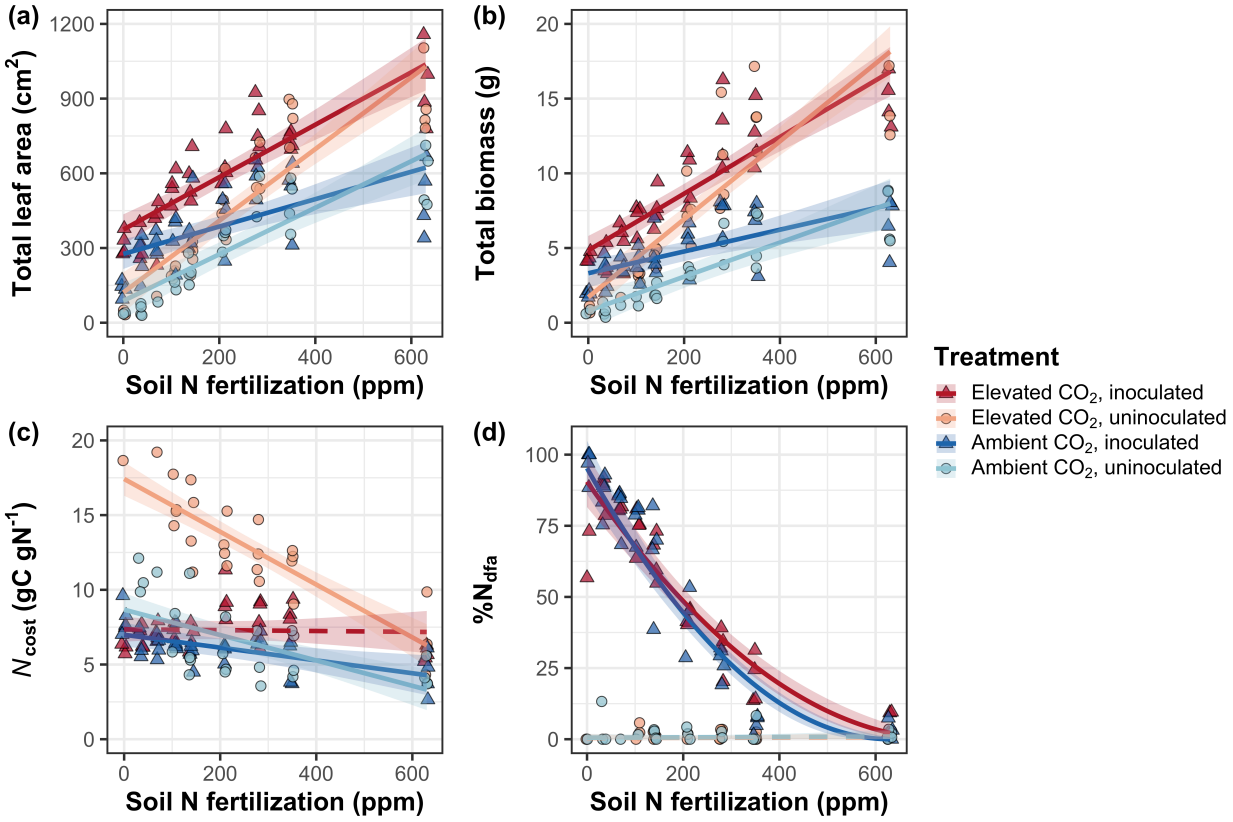

Figure 4. Effects of CO_2, nitrogen fertilization, and inoculation on total leaf area (a), total biomass (b), structural carbon costs to acquire nitrogen (c), and percent of leaf nitrogen content acquired from the atmosphere (d). Nitrogen fertilization is represented on the x-axis. Red shaded points and trendlines indicate plants grown under elevated CO_2, while blue shaded points and trendlines indicate plants grown under ambient CO_2. Light blue and red circular points and trendlines indicate measurements collected from uninoculated plants, while dark blue and red triangular points indicate measurements collected from inoculated plants. Solid trendlines indicate regression slopes that are different from zero ($p<0.05$), while dashed trendlines indicate slopes that are not distinguishable from zero ($p>0.05$).

578 **Discussion**

579 *Glycine max* seedlings were grown under two CO_2 concentrations, two inoculation treatments,
580 and nine soil nitrogen fertilization treatments in a full-factorial growth chamber experiment to
581 reconcile the role of nitrogen supply and demand on plant responses to elevated CO_2. Results
582 revealed that elevated CO_2 increased $A_{net,growth}$ despite reduced N_{area}, V_{cmax25}, and J_{max25}. Larger
583 reductions in V_{cmax25} than J_{max25} increased J_{max25}:V_{cmax25}, while respective increases and decreases
584 in $A_{net,growth}$ and N_{area} increased photosynthetic nitrogen-use efficiency. Effects of elevated CO_2
585 on $A_{net,growth}$, V_{cmax25}, J_{max25}, and J_{max25}:V_{cmax25} were each similar across the nitrogen fertilization
586 gradient, suggesting that leaf photosynthetic responses to elevated CO_2 were decoupled from
587 changes in nitrogen supply. Instead, increased J_{max25}:V_{cmax25} under elevated CO_2 indicated that
588 plants responded to increasing atmospheric CO_2 concentrations by allowing enhanced net
589 photosynthesis rates to be achieved by approaching equal co-limitation of Rubisco carboxylation
590 rate-limited photosynthesis and electron transport for RuBP regeneration rate-limited
591 photosynthesis (Chen *et al.*, 1993; Maire *et al.*, 2012). These responses supported our hypothesis
592 that leaf photosynthetic responses to elevated CO_2 would be driven by leaf nitrogen demand to
593 build and maintain photosynthetic enzymes. Leaf photosynthetic responses corresponded with
594 increased total leaf area and total biomass under elevated CO_2 that was generally enhanced with
595 increasing nitrogen fertilization, supporting our hypothesis that whole-plant responses to
596 elevated CO_2 would be constrained by nitrogen supply. Inoculation did not enhance whole-plant
597 responses to elevated CO_2 due to similar plant investment in symbiotic nitrogen fixation between
598 CO_2 treatments. These patterns, which were similar across the nitrogen fertilization gradient,
599 contrasted our hypothesis that inoculation would increase the positive whole-plant responses to
600 elevated CO_2 under low nitrogen fertilization.

601 Combined, results indicate that nitrogen supply and demand are each important factors
602 that drive plant responses to elevated CO_2 – leaf nitrogen demand to build and maintain
603 photosynthetic enzymes drove leaf photosynthetic responses to elevated CO_2, while nitrogen
604 supply constrained whole-plant growth responses to elevated CO_2. These findings strongly
605 support patterns expected from eco-evolutionary optimality theory, suggesting that terrestrial
606 biosphere models may improve simulations of leaf photosynthetic processes under future novel
607 environments by considering frameworks that adopt optimality principles (Smith & Keenan,

608 2020; Harrison *et al.*, 2021; Luo *et al.*, 2021). Below, we expand and contextualize these
609 conclusions and suggest their implications for terrestrial biosphere model development.
610
611 *Nitrogen supply and demand regulate leaf and whole-plant responses to elevated CO_2 at*
612 *different scales*
613 Leaf photosynthetic responses to elevated CO_2 were consistent with previous studies that have
614 investigated or reviewed leaf responses to elevated CO_2 (Drake *et al.*, 1997; Makino *et al.*, 1997;
615 Ainsworth *et al.*, 2002; Ainsworth & Long, 2005; Ainsworth & Rogers, 2007; Crous *et al.*, 2010;
616 Lee *et al.*, 2011; Smith & Dukes, 2013; Poorter *et al.*, 2022), and follow patterns expected from
617 eco-evolutionary optimality theory (Chen *et al.*, 1993; Wright *et al.*, 2003; Maire *et al.*, 2012;
618 Prentice *et al.*, 2014; Wang *et al.*, 2017; Smith *et al.*, 2019; Smith & Keenan, 2020; Harrison *et*
619 *al.*, 2021). Supporting eco-evolutionary optimality theory, positive effects of elevated CO_2 on
620 $A_{\mathrm{net,growth}}$ and J_{max25}:V_{cmax25} and negative effects of elevated CO_2 on V_{cmax25} and J_{max25} were
621 similar across the nitrogen fertilization gradient, suggesting that leaf photosynthetic responses to
622 elevated CO_2 were decoupled from changes in nitrogen supply. Instead, increased J_{max25}:V_{cmax25}
623 and photosynthetic nitrogen-use efficiency under elevated CO_2 provide strong support for the
624 idea that leaves were downregulating V_{cmax25} in response to elevated CO_2 such that enhanced net
625 photosynthesis rates approached becoming equally co-limited by Rubisco carboxylation and
626 RuBP regeneration (Chen *et al.*, 1993; Maire *et al.*, 2012; Smith & Keenan, 2020). These
627 patterns suggest that leaf photosynthetic responses to elevated CO_2 were the result of reduced
628 demand to build and maintain photosynthetic enzymes, as expected from eco-evolutionary
629 optimality theory (Harrison *et al.*, 2021; Dong *et al.*, 2022b).
630 Whole-plant responses were also consistent with previous studies that have investigated
631 or reviewed whole-plant responses to elevated CO_2 (Makino *et al.*, 1997; Ainsworth *et al.*, 2002;
632 Hungate *et al.*, 2003; Ainsworth & Long, 2005; Norby *et al.*, 2010; Smith & Dukes, 2013;
633 Poorter *et al.*, 2022). Greater whole-plant growth under elevated CO_2 was associated with greater
634 carbon costs to acquire nitrogen through stronger increases in belowground carbon allocation
635 than whole-plant nitrogen uptake. These patterns indicate that plants grown under elevated CO_2
636 supported greater total leaf area and total biomass through increased plant nitrogen uptake,
637 though at reduced nitrogen uptake efficiency. Unlike leaf photosynthetic responses to elevated
638 CO_2, positive whole-plant responses to elevated CO_2 were enhanced with increasing nitrogen

639 fertilization, supporting our hypothesis that nitrogen supply would constrain whole-plant
640 responses to elevated CO_2 (Luo *et al.*, 2004; Finzi *et al.*, 2007). Positive effects of increasing
641 nitrogen fertilization on total leaf area and total biomass were associated with reductions in
642 carbon costs to acquire nitrogen, a pattern that was driven by stronger increases in whole-plant
643 nitrogen uptake than belowground carbon allocation (Perkowski *et al.*, 2021). While reductions
644 in carbon costs to acquire nitrogen due to increasing nitrogen fertilization were similar between
645 CO_2 treatments, increasing nitrogen fertilization increased whole-plant nitrogen uptake more
646 strongly under elevated CO_2. This pattern, coupled with similar effects of nitrogen fertilization
647 on belowground carbon allocation responses to elevated CO_2, indicates that stronger growth
648 responses to elevated CO_2 with increasing nitrogen fertilization were likely driven by enhanced
649 nitrogen uptake efficiency. These findings suggest that positive short-term effects of nitrogen
650 supply on whole-plant responses to elevated CO_2 are linked to reduced costs of acquiring
651 nitrogen and increased nitrogen uptake efficiency, supporting conclusions from Terrer *et al.*
652 (2018).
653 Our findings indicate that nitrogen supply and demand could each explain plant responses
654 to elevated CO_2, though operated at different scales. Specifically, leaf photosynthetic responses
655 were determined through nitrogen demand to build and maintain photosynthetic enzymes, while
656 whole-plant responses to elevated CO_2 were driven through changes in soil nitrogen supply.
657 Interestingly, optimized nitrogen allocation to photosynthetic capacity may have resulted in
658 nitrogen savings at the leaf level that could have maximized nitrogen allocation to growth.
659 Overall, results suggest that plants grown under elevated CO_2 responded to increased nitrogen
660 supply by increasing the number of optimally coordinated leaves and that the downregulation in
661 photosynthetic capacity under elevated CO_2 is not a direct response to changes in nitrogen
662 supply.
663
664 *Inoculation with symbiotic nitrogen-fixing bacteria does not modify leaf or whole-plant*
665 *responses to elevated CO_2*
666 Inoculation increased N_{area}, $A_{net,420}$, $A_{net,growth}$, V_{cmax25}, J_{max25}, photosynthetic nitrogen-use
667 efficiency, total leaf area, and total biomass, and decreased J_{max25}:V_{cmax25} and R_{d25}. These patterns
668 support previous literature suggesting that species which form associations with symbiotic
669 nitrogen-fixing bacteria often have increased leaf nitrogen content, photosynthetic capacity, and

growth compared to species that do not form such associations (Adams *et al.*, 2016; Bytnerowicz *et al.*, 2023). Positive effects of inoculation on leaf and whole-plant traits were strongest under low nitrogen fertilization and rapidly diminished with increasing nitrogen fertilization as investment in symbiotic nitrogen fixation decreased (Andrews *et al.*, 2011; Friel & Friesen, 2019; Perkowski *et al.*, 2021), supporting the idea that nitrogen fixation is a nutrient acquisition strategy that may confer competitive benefits for nitrogen-fixing species growing in low soil nitrogen environments (Rastetter *et al.*, 2001; Vitousek *et al.*, 2002). Despite this, inoculation did not modify effects of elevated CO_2 on V_{cmax25}, J_{max25}, J_{max25}:V_{cmax25}, photosynthetic nitrogen-use efficiency, total leaf area, or total biomass. These patterns corresponded with null effects of elevated CO_2 on $\%N_{dfa}$ and the ratio of root nodule biomass to root biomass, suggesting that null effects of inoculation on leaf and whole-plant responses to elevated CO_2 were primarily due to similar plant investments toward symbiotic nitrogen fixation between CO_2 treatments. Null inoculation effects on plant responses to elevated CO_2 were apparent across the nitrogen fertilization gradient, contrasting our hypothesis that inoculation would enhance whole-plant responses to elevated CO_2 under low nitrogen fertilization where individuals invested more strongly in symbiotic nitrogen fixation. These patterns also contrast previous work showing that inoculated *G. max* is more responsive to increasing atmospheric CO_2 concentrations (Ainsworth *et al.*, 2002) and that plant investment toward symbiotic nitrogen fixation tends to be greater under scenarios that increase demand to acquire nitrogen (Friel & Friesen, 2019).

Implications for future model development

Many terrestrial biosphere models predict photosynthetic capacity through parameterized relationships between N_{area} and V_{cmax} (Rogers, 2014; Rogers *et al.*, 2017), which assumes that leaf nitrogen-photosynthesis relationships are constant across growing environments. Our results build on previous work suggesting that leaf nitrogen-photosynthesis relationships dynamically change across growing environments (Smith & Keenan, 2020; Luo *et al.*, 2021; Dong *et al.*, 2022b; Waring *et al.*, 2023), as elevated CO_2 reduced leaf nitrogen content more strongly than it increased $A_{net,growth}$ and decreased V_{cmax25} and J_{max25}. Additionally, positive effects of nitrogen fertilization on indices of photosynthetic capacity were only apparent in uninoculated plants, as there was no effect of nitrogen fertilization on V_{cmax25} or J_{max25} in inoculated plants regardless of CO_2 treatment. The positive effect of increasing nitrogen fertilization on N_{area} and Chl_{area} was

also markedly weaker in inoculated plants compared to uninoculated plants. These patterns indicate that leaf nitrogen-photosynthesis relationships are context-dependent on nitrogen acquisition strategy, may only be constant in environments where nitrogen supply limits leaf physiology, and will likely shift in response to increasing atmospheric CO_2 concentrations. Terrestrial biosphere models that predict photosynthetic capacity through parameterized relationships between N_{area} and V_{cmax} (e.g., Kattge *et al.*, 2009; Walker *et al.*, 2014) may risk overestimating photosynthetic capacity, therefore net primary productivity and the magnitude of the land carbon sink, under future novel growth environments.

Our results demonstrate that optimal resource allocation to photosynthetic capacity defines leaf photosynthetic responses to elevated CO_2 and that these responses are independent of nitrogen supply. Current approaches for simulating photosynthetic responses to CO_2 in terrestrial biosphere models that couple carbon and nitrogen cycles often invoke patterns expected from progressive nitrogen limitation, where photosynthetic responses to elevated CO_2 are modeled as a function of positive relationships between nitrogen availability and leaf nitrogen content. Our results contradict this framework, suggesting that photosynthetic responses to elevated CO_2 are driven by optimal nitrogen investment to satisfy leaf nitrogen demand to build and maintain photosynthetic enzymes. Optimality models that use principles from optimal coordination and photosynthetic least-cost theories (Wang *et al.*, 2017; Stocker *et al.*, 2020; Scott & Smith, 2022) are capable of capturing responses to CO_2 independent of nitrogen supply (Smith & Keenan, 2020; Harrison *et al.*, 2021), suggesting that the implementation of optimality frameworks in terrestrial biosphere models may improve the accuracy by which models simulate photosynthetic processes with increasing atmospheric CO_2 concentrations.

Previous work has highlighted that pot experiments which restrict belowground rooting volume may alter plant responses to environmental change (Ainsworth *et al.*, 2002; Poorter *et al.*, 2012). In this study, the ratio of pot volume to total biomass was greater under elevated CO_2 and increased with increasing nitrogen fertilization such that several treatment combinations exceeded the 1 g L^{-1} ratio recommended by Poorter *et al*. (2012) to avoid growth limitation imposed by restricted pot volume (Table S6; Fig. S6). While possible that pot size may have limited plant responses to elevated CO_2, similar responses to elevated CO_2 have been observed using field measurements that do not restrict belowground rooting volume (Bernacchi *et al.*, 2005; Crous *et al.*, 2010; Lee *et al.*, 2011; Pastore *et al.*, 2019; Smith & Keenan, 2020).

Additionally, we did not observe strong evidence for saturating effects of increasing fertilization on total biomass, belowground carbon biomass, or root biomass under conditions where biomass: pot volume ratios exceeded 1 g L^{-1} (e.g., individuals of either inoculation status grown under high fertilization and elevated CO_2), which would be expected if pot volume had limited plant growth. The lack of such responses indicate that the pot volume used in this study (6 L) was sufficient to avoid growth limitation.

Conclusions

Our results indicate that nitrogen supply and demand each helped explain plant responses to elevated CO_2, though operated at different scales. Supporting eco-evolutionary optimality theory, leaf photosynthetic responses to elevated CO_2 were independent of soil nitrogen supply and ability to associate with symbiotic nitrogen-fixing bacteria and were instead driven by leaf nitrogen demand to build and maintain photosynthetic enzymes such that net photosynthesis rates approached optimal coordination. Supporting the progressive nitrogen limitation hypothesis, whole-plant responses to elevated CO_2 were enhanced with increasing nitrogen fertilization due to increased plant nitrogen uptake efficiency coupled with possible cascading effects of nitrogen savings at the leaf level that may have maximized nitrogen allocation to whole-plant growth. However, inoculation did not modify whole-plant responses to elevated CO_2, as plants invested similarly in symbiotic nitrogen fixation between CO_2 treatments. Our findings suggest that plants grown under elevated CO_2 responded to increased nitrogen supply by increasing the number of optimally coordinated leaves and that the downregulation in photosynthetic capacity under elevated CO_2 was not a direct response to changes in nitrogen supply. The differential role of nitrogen supply on leaf and whole-plant responses to elevated CO_2 coupled with dynamic leaf nitrogen-photosynthesis relationships across CO_2 and nitrogen fertilization treatments suggests that terrestrial biosphere models may improve simulations of photosynthetic responses to increasing atmospheric CO_2 concentrations by adopting frameworks that include optimality principles.

Conflicts of Interest

The authors declare no conflicts of interest.

Acknowledgements

This study is a contribution to the LEMONTREE (Land Ecosystem Models based On New Theory, obseRvations and ExperimEnts) project, funded through the generosity of Eric and Wendy Schmidt by recommendation of the Schmidt Futures programme. EAP acknowledges support from a Texas Tech University Doctoral Dissertation Completion Fellowship and a Botanical Society of America Graduate Student Research Award. This work was also supported by US National Science Foundation awards to NGS (DEB-2045968 and DEB-2217353).

Data Availability

All R scripts, data, and metadata are available at https://doi.org/10.5281/zenodo.10177575 (or on GitHub at: https://github.com/eaperkowski/NxCO2xI_ms_data)

Author contributions

EAP conceptualized the study objectives and designed the experiment, collected data, conducted data analysis, and wrote the first manuscript draft. EE assisted with data collection and experiment maintenance. NGS conceptualized study objectives and experimental design with EAP and oversaw experiment progress. All authors provided manuscript feedback.

References

Adams MA, Turnbull TL, Sprent JI, Buchmann N. **2016**. Legumes are different: Leaf nitrogen, photosynthesis, and water use efficiency. *Proceedings of the National Academy of Sciences of the United States of America* **113**: 4098–4103.

Ainsworth EA, Davey PA, Bernacchi CJ, Dermody OC, Heaton EA, Moore DJ, Morgan PB, Naidu SL, Ra HSY, Zhu XG, *et al.* 2002. A meta-analysis of elevated [CO_2] effects on soybean (*Glycine max*) physiology, growth and yield. *Global Change Biology* **8**: 695–709.

Ainsworth EA, Long SP. **2005**. What have we learned from 15 years of free-air CO_2 enrichment (FACE)? A meta-analytic review of the responses of photosynthesis, canopy properties and plant production to rising CO_2. *New Phytologist* **165**: 351–372.

Ainsworth EA, Rogers A. **2007**. The response of photosynthesis and stomatal conductance to rising [CO_2]: mechanisms and environmental interactions. *Plant, Cell & Environment* **30**: 258–

270.

Allen K, Fisher JB, Phillips RP, Powers JS, Brzostek ER. **2020**. Modeling the carbon cost of plant nitrogen and phosphorus uptake across temperate and tropical forests. *Frontiers in Forests and Global Change* **3**: 1–12.

Andrews M, James EK, Sprent JI, Boddey RM, Gross E, dos Reis FB. **2011**. Nitrogen fixation in legumes and actinorhizal plants in natural ecosystems: Values obtained using ^{15}N natural abundance. *Plant Ecology and Diversity* **4**: 117–130.

Arora VK, Katavouta A, Williams RG, Jones CD, Brovkin V, Friedlingstein P, Schwinger J, Bopp L, Boucher O, Cadule P, *et al.* 2020. Carbon-concentration and carbon-climate feedbacks in CMIP6 models and their comparison to CMIP5 models. *Biogeosciences* **17**: 4173–4222.

Barnes JD, Balaguer L, Manrique E, Elvira S, Davison AW. **1992**. A reappraisal of the use of DMSO for the extraction and determination of chlorophylls a and b in lichens and higher plants. *Environmental and Experimental Botany* **32**: 85–100.

Bates D, Mächler M, Bolker B, Walker S. **2015**. Fitting linear mixed-effects models using lme4. *Journal of Statistical Software* **67**: 1–48.

Bernacchi CJ, Morgan PB, Ort DR, Long SP. **2005**. The growth of soybean under free air [CO_2] enrichment (FACE) stimulates photosynthesis while decreasing in vivo Rubisco capacity. *Planta* **220**: 434–446.

Bernacchi CJ, Singsaas EL, Pimentel C, Portis AR, Long SP. **2001**. Improved temperature response functions for models of Rubisco-limited photosynthesis. *Plant, Cell and Environment* **24**: 253–259.

Braghiere RK, Fisher JB, Allen K, Brzostek ER, Shi M, Yang X, Ricciuto DM, Fisher RA, Zhu Q, Phillips RP. **2022**. Modeling global carbon costs of plant nitrogen and phosphorus acquisition. *Journal of Advances in Modeling Earth Systems* **14**: 1–23.

Brzostek ER, Fisher JB, Phillips RP. **2014**. Modeling the carbon cost of plant nitrogen acquisition: Mycorrhizal trade-offs and multipath resistance uptake improve predictions of retranslocation. *Journal of Geophysical Research: Biogeosciences* **119**: 1684–1697.

Bytnerowicz TA, Funk JL, Menge DNL, Perakis SS, Wolf AA. **2023**. Leaf nitrogen affects photosynthesis and water use efficiency similarly in nitrogen-fixing and non-fixing trees. *Journal of Ecology*: 1–15.

824 **Chen J-L, Reynolds JF, Harley PC, Tenhunen JD**. **1993**. Coordination theory of leaf nitrogen
825 distribution in a canopy. *Oecologia* **93**: 63–69.
826 **Coleman JS, McConnaughay KDM, Bazzaz FA**. **1993**. Elevated CO_2 and plant nitrogen-use:
827 is reduced tissue nitrogen concentration size-dependent? *Oecologia* **93**: 195–200.
828 **Crous KY, Reich PB, Hunter MD, Ellsworth DS**. **2010**. Maintenance of leaf N controls the
829 photosynthetic CO_2 response of grassland species exposed to 9 years of free-air CO_2 enrichment.
830 *Global Change Biology* **16**: 2076–2088.
831 **Cui E, Xia J, Luo Y**. **2023**. Nitrogen use strategy drives interspecific differences in plant
832 photosynthetic CO_2 acclimation. *Global Change Biology* **29**: 3667–3677.
833 **Curtis PS**. **1996**. A meta-analysis of leaf gas exchange and nitrogen in trees grown under
834 elevated carbon dioxide. *Plant, Cell and Environment* **19**: 127–137.
835 **Davies-Barnard T, Meyerholt J, Zaehle S, Friedlingstein P, Brovkin V, Fan Y, Fisher RA,**
836 **Jones CD, Lee H, Peano D, *et al.* 2020**. Nitrogen cycling in CMIP6 land surface models:
837 progress and limitations. *Biogeosciences* **17**: 5129–5148.
838 **Dong N, Prentice IC, Evans BJ, Caddy-Retalic S, Lowe AJ, Wright IJ**. **2017**. Leaf nitrogen
839 from first principles: field evidence for adaptive variation with climate. *Biogeosciences* **14**: 481–
840 495.
841 **Dong N, Prentice IC, Wright IJ, Evans BJ, Togashi HF, Caddy-Retalic S, McInerney FA,**
842 **Sparrow B, Leitch E, Lowe AJ**. **2020**. Components of leaf-trait variation along environmental
843 gradients. *New Phytologist* **228**: 82–94.
844 **Dong N, Prentice IC, Wright IJ, Wang H, Atkin OK, Bloomfield KJ, Domingues TF,**
845 **Gleason SM, Maire V, Onoda Y, *et al.* 2022a**. Leaf nitrogen from the perspective of optimal
846 plant function. *Journal of Ecology* **110**: 2585–2602.
847 **Dong N, Wright IJ, Chen JM, Luo X, Wang H, Keenan TF, Smith NG, Prentice IC**. **2022b**.
848 Rising CO_2 and warming reduce global canopy demand for nitrogen. *New Phytologist* **235**:
849 1692–1700.
850 **Drake BG, Gonzàlez-Meler MA, Long SP**. **1997**. More efficient plants: a consequence of
851 rising atmospheric CO_2? *Annual Review of Plant Biology* **48**: 609–639.
852 **Duursma RA**. **2015**. Plantecophys - an R package for analysing and modelling leaf gas
853 exchange data. *PLOS ONE* **10**: e0143346.
854 **Evans JR**. **1989**. Photosynthesis and nitrogen relationships in leaves of C_3 plants. *Oecologia* **78**:

9–19.

Evans JR, Clarke VC. **2019**. The nitrogen cost of photosynthesis. *Journal of Experimental Botany* **70**: 7–15.

Evans JR, Seemann JR. **1989**. The allocation of protein nitrogen in the photosynthetic apparatus: costs, consequences, and control. *Photosynthesis* **8**: 183–205.

Farquhar GD, von Caemmerer S, Berry JA. **1980**. A biochemical model of photosynthetic CO_2 assimilation in leaves of C_3 species. *Planta* **149**: 78–90.

Farquhar GD, Ehleringer JR, Hubick KT. **1989**. Carbon isotope discrimination and photosynthesis. *Annual Review of Plant Physiology and Plant Molecular Biology* **40**: 503–537.

Fay PA, Prober SM, Harpole WS, Knops JMH, Bakker JD, Borer ET, Lind EM, MacDougall AS, Seabloom EW, Wragg PD, *et al.* 2015. Grassland productivity limited by multiple nutrients. *Nature Plants* **1**: 15080.

Field CB, Mooney HA. **1986**. The photosynthesis-nitrogen relationship in wild plants. In: Givnish TJ, ed. On the Economy of Plant Form and Function. Cambridge: Cambridge University Press, 25–55.

Finzi AC, Moore DJP, DeLucia EH, Lichter J, Hofmockel KS, Jackson RB, Kim HS, Matamala R, McCarthy HR, Oren R, *et al.* 2006. Progressive nitrogen limitation of ecosystem processes under elevated CO_2 in a warm-temperate forest. *Ecology* **87**: 15–25.

Finzi AC, Norby RJ, Calfapietra C, Gallet-Budynek A, Gielen B, Holmes WE, Hoosbeek MR, Iversen CM, Jackson RB, Kubiske ME, *et al.* 2007. Increases in nitrogen uptake rather than nitrogen-use efficiency support higher rates of temperate forest productivity under elevated CO_2. *Proceedings of the National Academy of Sciences* **104**: 14014–14019.

Firn J, McGree JM, Harvey E, Flores-Moreno H, Schütz M, Buckley YM, Borer ET, Seabloom EW, La Pierre KJ, MacDougall AM, *et al.* 2019. Leaf nutrients, not specific leaf area, are consistent indicators of elevated nutrient inputs. *Nature Ecology & Evolution* **3**: 400–406.

Fox J, Weisberg S. **2019**. *An R companion to applied regression*. Thousand Oaks, California: Sage.

Friedlingstein P, Meinshausen M, Arora VK, Jones CD, Anav A, Liddicoat SK, Knutti R. **2014**. Uncertainties in CMIP5 climate projections due to carbon cycle feedbacks. *Journal of Climate* **27**: 511–526.

Friel CA, Friesen ML. **2019**. Legumes modulate allocation to rhizobial nitrogen fixation in response to factorial light and nitrogen manipulation. *Frontiers in Plant Science* **10**: 1316.

Gutschick VP. **1981**. Evolved strategies in nitrogen acquisition by plants. *The American Naturalist* **118**: 607–637.

Harrison SP, Cramer W, Franklin O, Prentice IC, Wang H, Brännström Å, de Boer H, Dieckmann U, Joshi J, Keenan TF, *et al.* 2021. Eco-evolutionary optimality as a means to improve vegetation and land-surface models. *New Phytologist* **231**: 2125–2141.

Hoagland DR, Arnon DI. **1950**. The water-culture method for growing plants without soil. *California Agricultural Experiment Station: 347* **347**: 1–32.

Hungate BA, Dukes JS, Shaw MR, Luo Y, Field CB. **2003**. Nitrogen and climate change. *Science* **302**: 1512–1513.

Katabuchi M. **2015**. LeafArea: An R package for rapid digital analysis of leaf area. *Ecological Research* **30**: 1073–1077.

Kattge J, Knorr W, Raddatz T, Wirth C. **2009**. Quantifying photosynthetic capacity and its relationship to leaf nitrogen content for global-scale terrestrial biosphere models. *Global Change Biology* **15**: 976–991.

Kenward MG, Roger JH. **1997**. Small sample inference for fixed effects from restricted maximum likelihood. *Biometrics* **53**: 983.

Kou-Giesbrecht S, Arora VK, Seiler C, Arneth A, Falk S, Jain AK, Joos F, Kennedy D, Knauer J, Sitch S, *et al.* 2023. Evaluating nitrogen cycling in terrestrial biosphere models: a disconnect between the carbon and nitrogen cycles. *Earth System Dynamics* **14**: 767–795.

LeBauer DS, Treseder K. **2008**. Nitrogen limitation of net primary productivity in terrestrial ecosystems is globally distributed. *Ecology* **89**: 371–379.

Lee TD, Barrott SH, Reich PB. **2011**. Photosynthetic responses of 13 grassland species across 11 years of free-air CO_2 enrichment is modest, consistent and independent of N supply. *Global Change Biology* **17**: 2893–2904.

Lenth R. **2019**. emmeans: estimated marginal means, aka least-squares means.

Liang J, Qi X, Souza L, Luo Y. **2016**. Processes regulating progressive nitrogen limitation under elevated carbon dioxide: a meta-analysis. *Biogeosciences* **13**: 2689–2699.

Liang X, Zhang T, Lu X, Ellsworth DS, BassiriRad H, You C, Wang D, He P, Deng Q, Liu H, *et al.* 2020. Global response patterns of plant photosynthesis to nitrogen addition: A meta-

917 analysis. *Global Change Biology* **26**: 3585–3600.
918 **Luo Y, Currie WS, Dukes JS, Finzi AC, Hartwig UA, Hungate BA, McMurtrie RE, Oren**
919 **R, Parton WJ, Pataki DE, *et al.* 2004**. Progressive nitrogen limitation of ecosystem responses
920 to rising atmospheric carbon dioxide. *BioScience* **54**: 731–739.
921 **Luo Y, Field CB, Mooney HA**. **1994**. Predicting responses of photosynthesis and root fraction
922 to elevated [CO_2]: interactions among carbon, nitrogen, and growth. *Plant, Cell & Environment*
923 **17**: 1195–1204.
924 **Luo X, Keenan TF, Chen JM, Croft H, Prentice IC, Smith NG, Walker AP, Wang H, Wang**
925 **R, Xu C, *et al.* 2021**. Global variation in the fraction of leaf nitrogen allocated to photosynthesis.
926 *Nature Communications* **12**: 4866.
927 **Maire V, Martre P, Kattge J, Gastal F, Esser G, Fontaine S, Soussana J-F**. **2012**. The
928 coordination of leaf photosynthesis links C and N fluxes in C_3 plant species. *PLoS ONE* **7**:
929 e38345.
930 **Makino A, Harada M, Sato T, Nakano H, Mae T**. **1997**. Growth and N allocation in rice
931 plants under CO_2 enrichment. *Plant Physiology* **115**: 199–203.
932 **Medlyn BE, Badeck FW, De Pury DGG, Barton CVM, Broadmeadow M, Ceulemans R, De**
933 **Angelis P, Forstreuter M, Jach ME, Kellomäki S, *et al.* 1999**. Effects of elevated [CO_2] on
934 photosynthesis in European forest species: A meta-analysis of model parameters. *Plant, Cell and*
935 *Environment* **22**: 1475–1495.
936 **Meyerholt J, Sickel K, Zaehle S**. **2020**. Ensemble projections elucidate effects of uncertainty in
937 terrestrial nitrogen limitation on future carbon uptake. *Global Change Biology* **26**: 3978–3996.
938 **Moore DJP, Aref S, Ho RM, Pippen JS, Hamilton JG, De Lucia EH**. **2006**. Annual basal area
939 increment and growth duration of *Pinus taeda* in response to eight years of free-air carbon
940 dioxide enrichment. *Global Change Biology* **12**: 1367–1377.
941 **Nie M, Lu M, Bell J, Raut S, Pendall E**. **2013**. Altered root traits due to elevated CO_2: A meta-
942 analysis. *Global Ecology and Biogeography* **22**: 1095–1105.
943 **Norby RJ, Warren JM, Iversen CM, Medlyn BE, McMurtrie RE**. **2010**. CO_2 enhancement
944 of forest productivity constrained by limited nitrogen availability. *Proceedings of the National*
945 *Academy of Sciences* **107**: 19368–19373.
946 **Oreskes N, Shrader-Frechette K, Belitz K**. **1994**. Verification, validation, and confirmation of
947 numerical models in the Earth sciences. *Science* **263**: 641–646.

Paillassa J, Wright IJ, Prentice IC, Pepin S, Smith NG, Ethier G, Westerband AC, Lamarque LJ, Wang H, Cornwell WK, *et al.* 2020. When and where soil is important to modify the carbon and water economy of leaves. *New Phytologist* **228**: 121–135.

Pastore MA, Lee TD, Hobbie SE, Reich PB. **2019**. Strong photosynthetic acclimation and enhanced water-use efficiency in grassland functional groups persist over 21 years of CO_2 enrichment, independent of nitrogen supply. *Global Change Biology* **25**: 3031–3044.

Peng Y, Bloomfield KJ, Cernusak LA, Domingues TF, Prentice IC. **2021**. Global climate and nutrient controls of photosynthetic capacity. *Communications Biology* **4**: 462.

Peng Y, Prentice IC, Bloomfield KJ, Campioli M, Guo Z, Sun Y, Tian D, Wang X, Vicca S, Stocker BD. **2023**. Global terrestrial nitrogen uptake and nitrogen use efficiency. *Journal of Ecology*: 1–18.

Perkowski EA, Waring EF, Smith NG. **2021**. Root mass carbon costs to acquire nitrogen are determined by nitrogen and light availability in two species with different nitrogen acquisition strategies. *Journal of Experimental Botany* **72**: 5766–5776.

Poorter H, Bühler J, Van Dusschoten D, Climent J, Postma JA. **2012**. Pot size matters: A meta-analysis of the effects of rooting volume on plant growth. *Functional Plant Biology* **39**: 839–850.

Poorter H, Knopf O, Wright IJ, Temme AA, Hogewoning SW, Graf A, Cernusak LA, Pons TL. **2022**. A meta-analysis of responses of C_3 plants to atmospheric CO_2: dose–response curves for 85 traits ranging from the molecular to the whole-plant level. *New Phytologist* **233**: 1560–1596.

Prentice IC, Dong N, Gleason SM, Maire V, Wright IJ. **2014**. Balancing the costs of carbon gain and water transport: testing a new theoretical framework for plant functional ecology. *Ecology Letters* **17**: 82–91.

Prentice IC, Liang X, Medlyn BE, Wang Y-P. **2015**. Reliable, robust and realistic: The three R's of next-generation land-surface modelling. *Atmospheric Chemistry and Physics* **15**: 5987–6005.

Querejeta JI, Prieto I, Armas C, Casanoves F, Diémé JS, Diouf M, Yossi H, Kaya B, Pugnaire FI, Rusch GM. **2022**. Higher leaf nitrogen content is linked to tighter stomatal regulation of transpiration and more efficient water use across dryland trees. *New Phytologist* **235**: 1351–1364.

R Core Team. **2021**. R: A language and environment for statistical computing.

Rastetter EB, Vitousek PM, Field CB, Shaver GR, Herbert D, Ågren GI. **2001**. Resource optimization and symbiotic nitrogen fixation. *Ecosystems* **4**: 369–388.

Reich PB, Hobbie SE, Lee T, Ellsworth DS, West JB, Tilman D, Knops JMH, Naeem S, Trost J. **2006**. Nitrogen limitation constrains sustainability of ecosystem response to CO_2. *Nature* **440**: 922–925.

Rogers A. **2014**. The use and misuse of $V_{c,max}$ in Earth System Models. *Photosynthesis Research* **119**: 15–29.

Rogers A, Medlyn BE, Dukes JS, Bonan GB, Caemmerer S, Dietze MC, Kattge J, Leakey ADB, Mercado LM, Niinemets Ü, *et al.* 2017. A roadmap for improving the representation of photosynthesis in Earth system models. *New Phytologist* **213**: 22–42.

Saathoff AJ, Welles J. **2021**. Gas exchange measurements in the unsteady state. *Plant Cell and Environment* **44**: 3509–3523.

Sage RF. **1994**. Acclimation of photosynthesis to increasing atmospheric CO_2: The gas exchange perspective. *Photosynthesis Research* **39**: 351–368.

Schneider CA, Rasband WS, Eliceiri KW. **2012**. NIH Image to ImageJ: 25 years of image analysis. *Nature Methods* **9**: 671–675.

Scott HG, Smith NG. **2022**. A Model of C4 Photosynthetic Acclimation Based on Least-Cost Optimality Theory Suitable for Earth System Model Incorporation. *Journal of Advances in Modeling Earth Systems* **14**: 1–16.

Shi M, Fisher JB, Brzostek ER, Phillips RP. **2016**. Carbon cost of plant nitrogen acquisition: Global carbon cycle impact from an improved plant nitrogen cycle in the Community Land Model. *Global Change Biology* **22**: 1299–1314.

Smith NG, Dukes JS. **2013**. Plant respiration and photosynthesis in global-scale models: incorporating acclimation to temperature and CO_2. *Global Change Biology* **19**: 45–63.

Smith NG, Keenan TF. **2020**. Mechanisms underlying leaf photosynthetic acclimation to warming and elevated CO_2 as inferred from least-cost optimality theory. *Global Change Biology* **26**: 5202–5216.

Smith NG, Keenan TF, Prentice IC, Wang H, Wright IJ, Niinemets Ü, Crous KY, Domingues TF, Guerrieri R, Ishida FY, *et al.* 2019. Global photosynthetic capacity is optimized to the environment. *Ecology Letters* **22**: 506–517.

Smith SE, Read DJ. **2008**. *Mycorrhizal Symbiosis*.

Stocker BD, Wang H, Smith NG, Harrison SP, Keenan TF, Sandoval D, Davis T, Prentice IC. **2020**. P-model v1.0: An optimality-based light use efficiency model for simulating ecosystem gross primary production. *Geoscientific Model Development* **13**: 1545–1581.

Terrer C, Vicca S, Hungate BA, Phillips RP, Prentice IC. **2016**. Mycorrhizal association as a primary control of the CO_2 fertilization effect. *Science* **353**: 72–74.

Terrer C, Vicca S, Stocker BD, Hungate BA, Phillips RP, Reich PB, Finzi AC, Prentice IC. **2018**. Ecosystem responses to elevated CO_2 governed by plant–soil interactions and the cost of nitrogen acquisition. *New Phytologist* **217**: 507–522.

Vitousek PM, Cassman K, Cleveland CC, Crews T, Field CB, Grimm NB, Howarth RW, Marino R, Martinelli L, Rastetter EB, *et al.* 2002. Towards an ecological understanding of biological nitrogen fixation. In: The Nitrogen Cycle at Regional to Global Scales. Dordrecht: Springer Netherlands, 1–45.

Vitousek PM, Howarth RW. **1991**. Nitrogen limitation on land and in the sea: How can it occur? *Biogeochemistry* **13**: 87–115.

Walker AP, Beckerman AP, Gu L, Kattge J, Cernusak LA, Domingues TF, Scales JC, Wohlfahrt G, Wullschleger SD, Woodward FI. **2014**. The relationship of leaf photosynthetic traits - V_{cmax} and J_{max} - to leaf nitrogen, leaf phosphorus, and specific leaf area: a meta-analysis and modeling study. *Ecology and Evolution* **4**: 3218–3235.

Wang H, Prentice IC, Keenan TF, Davis TW, Wright IJ, Cornwell WK, Evans BJ, Peng C. **2017**. Towards a universal model for carbon dioxide uptake by plants. *Nature Plants* **3**: 734–741.

Waring EF, Perkowski EA, Smith NG. **2023**. Soil nitrogen fertilization reduces relative leaf nitrogen allocation to photosynthesis. *Journal of Experimental Botany* **74**: 5166–5180.

Wellburn AR. **1994**. The spectral determination of chlorophylls a and b, as well as total carotenoids, using various solvents with spectrophotometers of different resolution. *Journal of Plant Physiology* **144**: 307–313.

Westerband AC, Wright IJ, Maire V, Paillassa J, Prentice IC, Atkin OK, Bloomfield KJ, Cernusak LA, Dong N, Gleason SM, *et al.* 2023. Coordination of photosynthetic traits across soil and climate gradients. *Global Change Biology* **29**: 856–873.

Wieder WR, Cleveland CC, Smith WK, Todd-Brown K. **2015**. Future productivity and carbon storage limited by terrestrial nutrient availability. *Nature Geoscience* **8**: 441–444.

Wright IJ, Reich PB, Westoby M. **2003**. Least-cost input mixtures of water and nitrogen for photosynthesis. *The American Naturalist* **161**: 98–111.

Zaehle S, Medlyn BE, De Kauwe MG, Walker AP, Dietze MC, Hickler T, Luo Y, Wang YP, El-Masri B, Thornton P, *et al.* 2014. Evaluation of 11 terrestrial carbon-nitrogen cycle models against observations from two temperate Free-Air CO_2 Enrichment studies. *New Phytologist* **202**: 803–822.